Numerical modelling of wind-induced variability of hydrological parameters in the coastal zone of the Baltic Sea

Andrzej Jankowski

Institute of Oceanology.
Polish Academy of Sciences,
Powstańców Warszawy 55, 81-712 Sopot, Poland
jankowsk@iopan.gda.pl

Contents

Abstract

A three-dimensional σ-coordinate model based on the Princeton Ocean Model code (Mellor, 1993) was applied to study wind-induced variability of hydrological parameters in the Baltic Sea. The model comprises the whole Baltic with its main basins: the Gulf of Bothnia, the Gulf of Finland, the Gulf of Riga, the Belt Sea, Kattegat and Skagerrak. Model is forced with artificial forcings with three successive storms of constant speed. Variability of hydrological parameters in the coastal region of the southeast part of the Baltic Sea as a response of a stratified sea to an onset of variable winds are reported. Numerical experiments show that the winds from SE to NE form suitable condition to occurr coastal upwelling along the Polish Baltic coasts.

Key words: Baltic Sea, coastal area, numerical modelling, upwelling, variability of hydrological parameters

1. INTRODUCTION

The results of the baroclinic σ-coordinate numerical model based on the Princeton Ocean Model - code (hereafter POM) (**Blumberg and Mellor, 1987**; **Mellor, 1993**) applied to study wind- and density-driven circulation in the Baltic Sea are presented.

The model, with a horizontal resolution of $\sim$ 10 km and with 24 σ-levels in vertical, covers the Baltic Proper, the Gulfs of Bothnia, Finland and Riga as well as the Belt Sea, Kattegat and Skagerrak. At the open boundary in Skagerrak the simplified, radiation type, boundary conditions were applied.

The study is concentrated on single event; a model wind stress on the Baltic Sea was applied and the associated baroclinic response of stratified sea water was computed.

It will be shown that under the atmospheric forcing of three successive storms, near the southern Baltic coasts intensive upwelling/downwelling phenomena develop. This phenomenon, due to the variable wind conditions over the Baltic, constraint to its complicated bottom topography and configuration of shoreline, is frequently observed along its coasts (cf. e.g.: **Gidhagen, 1984**; **Bychkova and Viktorov, 1987**; **Bychkova et al., 1988**; **Urbański, 1995**; **Hansen et al., 1993**; **Haapala, 1994**; **Krężel, 1997**).

Presentation of results is limited to the coastal zone along the south coasts of the Baltic Sea (along the Polish Baltic coast). The charts of modeled sea water temperature as well as time evolution of calculated velocity components, sea water temperature and its salinity at the selected points are shown.

2. MODEL DESIGN

In recent years, the POM code has been extensively used to study water circulation in ocean and seas, among other, also in the Baltic Sea (cf. e.g., **Ezer and Mellor, 1994**; **Ezer and Mellor, 1997**; **Oey and Chen, 1992a**; **1992b**; **Svendsen et al., 1996**; **Jędrasik, 1997**; **Kowalewski, 1997**). However, it is necessary to note that for the Baltic Sea conditions, more frequently, z-level models, based on Bryan-Cox-Semtner model (cf. **Killworth et al., 1991**) are applied (e.g. cf.: **Krauss, 1991**; **Lehmann, 1995**; **Elken, 1996**; **Meier, 1999**; **Meier et al, 1999**; **Lehmann and Hinrichsen, 2000a**; **2000b**).

2.1. EQUATIONS AND BOUNDARY CONDITIONS

The Princeton Ocean Model (cf. **Blumberg and Mellor, 1987**; **Mellor, 1993**) is a fully three-dimensional numerical σ-level model and includes the necessary components in order to be able to reproduce the important physical features of the ocean circulation. The model is based on a standard formulation of the conservation equations for momentum and mass, utilizing the hydrostatic and the Boussinesq approximations and assuming the water masses to be incompressible:

$$\mathbf{u}_t + \mathbf{u}\cdot\nabla\mathbf{u} + w_z\mathbf{u}_z + f\mathbf{k}\times\mathbf{u} = -\frac{1}{\rho_0}\nabla p + (A_v\mathbf{u}_z)_z + \mathbf{F}, \tag{1}$$

$$p_z = -\rho g, \tag{2}$$

$$\Theta_t + \mathbf{u}\cdot\nabla\Theta + w_z\Theta_z = (K_v\Theta_z)_z + \nabla\cdot(K_H\nabla\Theta), \tag{3}$$

$$\nabla\cdot\mathbf{u} + w_z = 0; \quad \rho = \rho(T,S). \tag{4}$$

Here, $\mathbf{u}$ is the horizontal velocity vector, with components (u, v) and w is the vertical component. ∇ is the horizontal gradient operator, f is the Coriolis parameter, $\mathbf{k}$ is the vertical unit vector, ρ_0 is a reference density, p is the pressure, g is the gravitational acceleration, z is the vertical coordinate (positive upwards), Θ represents either sea water temperature T or its salinity S, A_v is the vertical eddy viscosity, K_v and K_H are associated vertical and horizontal eddy diffusivities, respectively. The water density ρ is related to salinity and temperature through an equation of state (4) in accordance with UNESCO standards (**UNESCO, 1983**). $\mathbf{F}$ refers to horizontal mixing term added to parametrize subgrid scale processes Subscripts z and t refer to a derivative with respect to the subscript (vertical coordinate and time, respectively).

Boundary conditions at the sea surface ($z = \eta$):

$$A_v(u_z, v_z) = (\tau_x^s, \tau_y^s); \quad K_v(T_z, S_z) = (Q_T, Q_S); \quad w = \eta_t + \mathbf{u} \cdot \nabla\eta, \tag{5}$$

where (τ_x^s, τ_y^s) are components of the wind stress vector and Q_T, Q_S are heat and salinity fluxes.

Boundary conditions at the sea bottom ($z = -H$):

$$A_v(u_z, v_z) = C_D|\mathbf{u}_b|\mathbf{u}_b; \quad K_v(T_z, S_z) = (0, 0); \quad w = -\mathbf{u} \cdot \nabla H. \tag{6}$$

Here, $\mathbf{u}_b$ is the horizontal velocity at the sea bottom, C_D is drag coefficient equal to 0.0025.

Boundary conditions at the lateral boundary ($(x, y) \in L$):

$$U_n = \frac{C_e}{H}\eta; \quad C_e = (gH)^{1/2}; \quad (\mathbf{n} \cdot \mathbf{u})_t + C_i(\mathbf{n} \cdot \mathbf{u})_n = 0; \quad (T, S)_t + |\mathbf{n} \cdot \mathbf{u}_n|(T, S)_n = 0. \tag{7}$$

Here, $\mathbf{n}$ is a unit outward vector normal to boundary line L, U_n is the depth-averaged velocity normal to the boundary, C_i is the internal phase speed taken to be a constant equal to $(gH \times 10^{-3})^{1/2}$.

2.2. MODEL PARAMETERS AND NUMERICAL SOLUTION

In the POM code, a second order turbulence closure scheme (**Mellor and Yamada, 1982**) is applied to estimate the vertical eddy viscosity and the vertical diffusion coefficients. It is based on an improved understanding of the physical processes related to the ocean turbulence and includes the set of equations for the turbulent energy and the turbulent macroscale (**Mellor and Yamada, 1982**; **Blumberg and Mellor, 1987**; **Mellor, 1993**).

Parametrization of the horizontal mixing in the POM model is based on the Smagorinsky formula (**Smagorinsky, 1963**):

$$\mathbf{F} = \nabla \cdot \begin{bmatrix} 2A_H u_x & A_H(u_x + v_y) \\ A_H(u_y + v_x) & 2A_H v_y \end{bmatrix}, \tag{8}$$

where coefficient A_H (and K_H) is given by the formula:

$$A_H = K_H = C\Delta x \Delta y \times [u_x^2 + v_y^2 + 0.5(u_y + v_x)^2]^{-1/2}, \tag{9}$$

where Δx and Δy are the horizontal grid distance and C is a numerical constant.

The governing equations and boundary conditions, prior to be discretized, are transformed from Cartesian coordinate system (x, y, z, t) to a terrain-following co-

ordinate system (commonly referred to as σ-coordinates) (x^1, y^1, σ, t^1):

$$x^1 = x; \quad y^1 = y; \quad \sigma = \frac{z - \eta}{H + \eta} \quad t^1 = t, \tag{10}$$

where η is the deviation of the free surface from its equilibrium position, $(z = 0)$ and H is the equilibrium depth of a water column.

The momentum and mass transport equations, after have been transformed to σ-coordinate system (10), are solved numerically by the finite - difference methods. The POM code uses an "Arakawa C" numerical grid (cf. **Mesinger and Arakawa, 1976**) and conserves both linear and quadratic quantities like mass, energy and vorticity. Time differencing is explit in the horizontal and implicit in vertical. Thus time constraints due to vertical grid are removed, permitting fine resolution in the surface and bottom boundary layers.

The model has a free surface and thus can include atmosperic induced sea level variations and free surface gavity waves. Time integrations is therefore split into a two-dimensional $(2 - D)$, external mode with a short time step based on the CFL's stability condition calculated using the (fastest) free surface gravity wave speed, and a three-dimensional $(3 - D)$, internal mode with a long time step based on the CFL's condition calculated using the internal wave speed.

Futher details concerning numerical schemes used in the POM code can be find in (**Mellor, 1993**).

In our calculations horizontal space steps of $\Delta\lambda = 10.8'$ and $\Delta\phi = 5.4'$ (i.e. grid size of $\sim$ 10 km) were used. In vertical, 24 σ-levels with distribution

$$(0.00000, -0.00329, -0.00658, -0.01316, -0.02632, -0.05263,$$
$$-0.10526, -0.15789, -0.21053, -0.26316, -0.31579, -0.36842,$$
$$-0.42105, -0.47368, -0.52632, -0.57895, -0.63158, -0.68421,$$
$$-0.73684, -0.78947, -0.84211, -0.89474, -0.94737, -1.00000).$$

were used. Time steps for the external $2-D$ and internal $3-D$ calculation mode were 10 sec. and 10 min., respectively.

3. NUMERICAL EXPERIMENTS AND SIMULATIONS

The calculations which results are presented here were carried out for summer (August) termohaline conditions (multi-year averaged, climatological conditions). Bottom topography of the Baltic Sea used in the model calculations is based on data from (**Seifert and Kayser, 1995**).

All numerical simulations of total duration of 50 days were performed in two stages. The first stage (days 0-20) was a semi-prognostic pre-processing run and the model was forced only by climatological forcings without wind stress. At the second stage, the model was forced so by climatological forcings as by atmospheric forcings.

The initial fields of sea level η, currents velocity vector component u, v, w and the mean-depth currents components U, V were set equal to 0. The three-dimensional fields of the sea water temperature T and its salinity S of August, constructed from the montly mean (multi-year averaged, climatic) maps presented in **Bock**'s (1971) and

Lenz's (1971) atlases, were used in model runs as initial fields of T, S. The surface distributions of temperature and salinity taken from **Bock**'s (1971) and **Lenz**'s (1971) atlases served as field of climatological forcing.

The climatological forcings were coupled to model by means of so-called method of "relaxtion towards climatology" (cf. e.g. **Oey and Chen, 1992a**; **Svendsen et al., 1996**; **Lehmann, 1995**) where the surface heat and salinity fluxes Q_T, Q_S (6) can be estimated as follows:

$$Q_T = C_{TC}(T_c - T); \quad Q_S = C_{SC}(S_c - S). \tag{11}$$

where C_{TC}, C_{SC} are the relaxation constants equal to $C_{TC}^{-1} = 2$ days and $C_{SC}^{-1} = 20$ days, respectively, T, S – calculated values of temperature and salinity at the first σ level, respectively, T_c, S_c – climatological values of temperature and salinity at the sea surface, respectively.

An adaption of the model dynamics to initial fields and climatology was achived by a forward integration of the model equations over a period of 20 days when a quasi-stationary state was reached.

The second stage (days 20-50) was initialized from the previous stage and consisted of a prognostic run when model was forced by both climatological forcings and by model atmospheric forcings (winds) of three successive storms.

Winds from main directions and of a constant speed over the Baltic during each storms were considered. Duration of each single storm was 5 days. In all cases the maximum wind stress applied was $\tau = 0.1 Nm^{-2}$. Example of wind time history during numerical simulations is presented in Fig. 1.

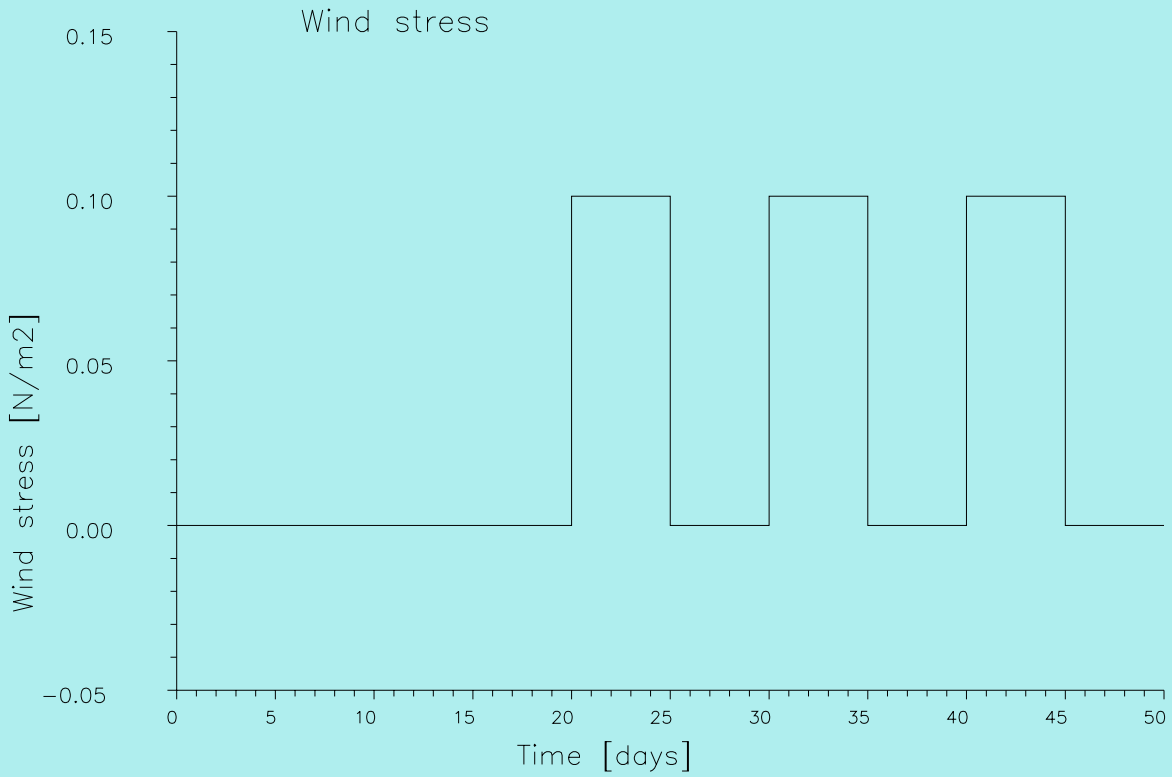

Figure 1: Time history of the wind stress applied in the model calculations.

4. RESULTS AND COMMENTS

Although model runs were performed for the entire Baltic Sea, for purpose of this study, presentation of results of simulation is limited to the southeast part of the Baltic Sea (12^o 30'E-21^o 30'E; 53^o 30'N-56^o 30'N) (cf. Fig. 2).

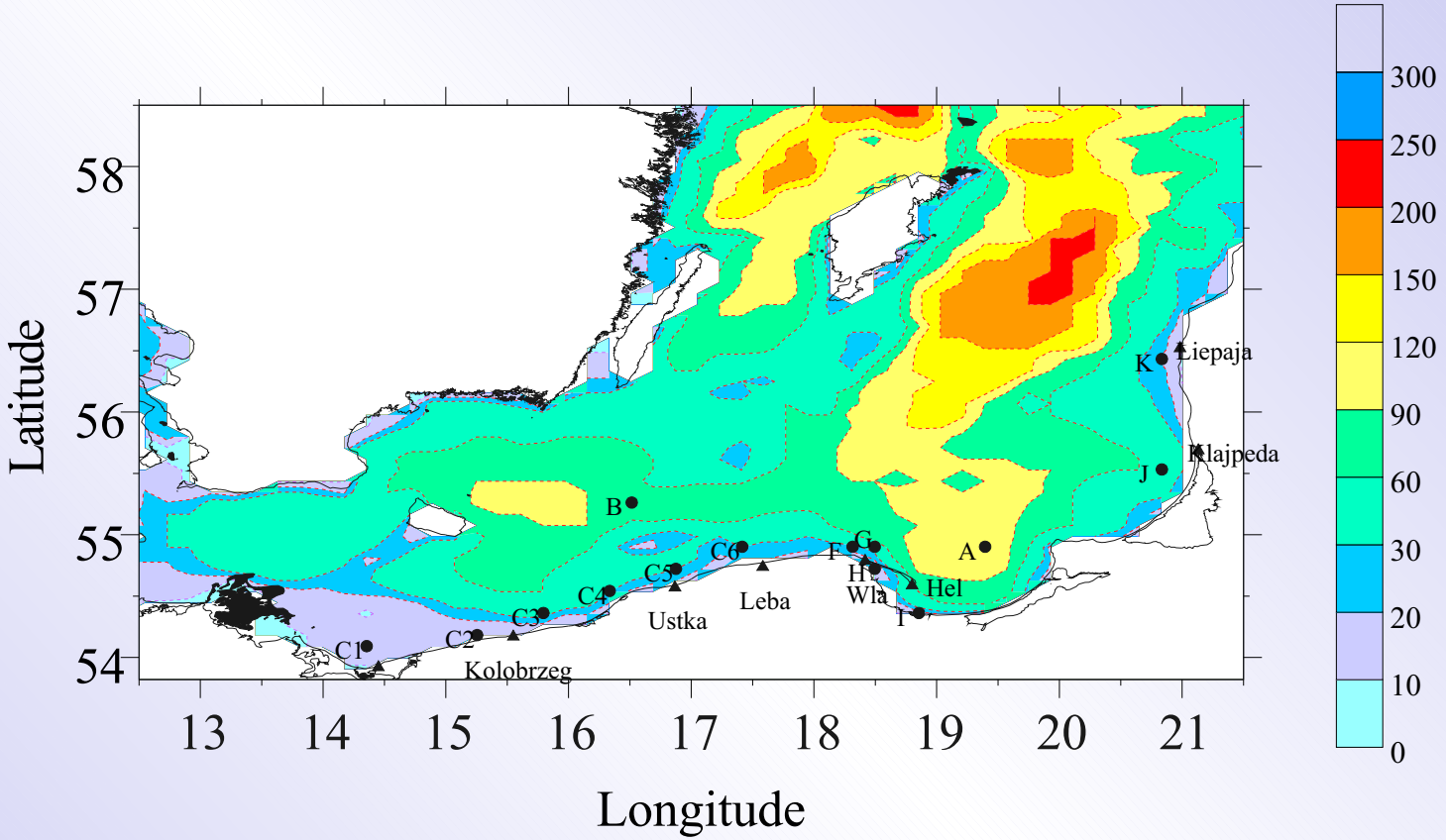

Figure 2: Bottom topography of the Southern Baltic Sea (based on data from Seifert and Kayser (1995) and locations of the selected points used for visualisation of time evolution of calculated hydrological parameters. Number on isobaths indicate sea depth in meters.

The time evolution of the modeled sea water temperature and its salinity at selected points along the Polish Baltic coasts are presented in Fig. 3 and Fig. 4. Location of the points is shown in Fig. 2. To test utility of POM code for the Baltic Sea conditions two cases of winds of opposite direction i.e., from the East and West, are considered. In order to complete the picture of hydrological, upwelling/downwelling-like, regime in coastal zone induced by fluctuating winds time evolution of zonal and meridional velocity components in points C4 and F are shown in Figs. 5 and 6 for the same wind conditions.

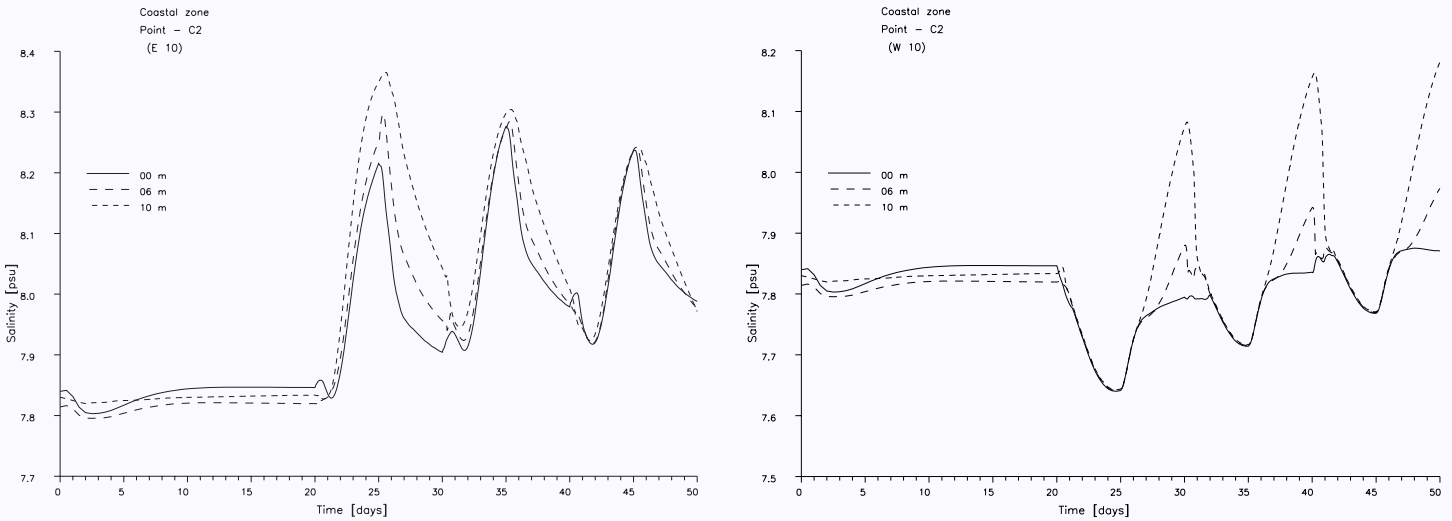

Figure 3: Time evolution of sea water salinity (psu) at the selected points in the southern Baltic Sea calculated for the case of storms with wind from East (left panel) and from West (right panel). a. point C2. Time course of wind stress is shown in Fig. 1. Location of points – see Fig. 2.

Figure 3 Continued b. point C4.

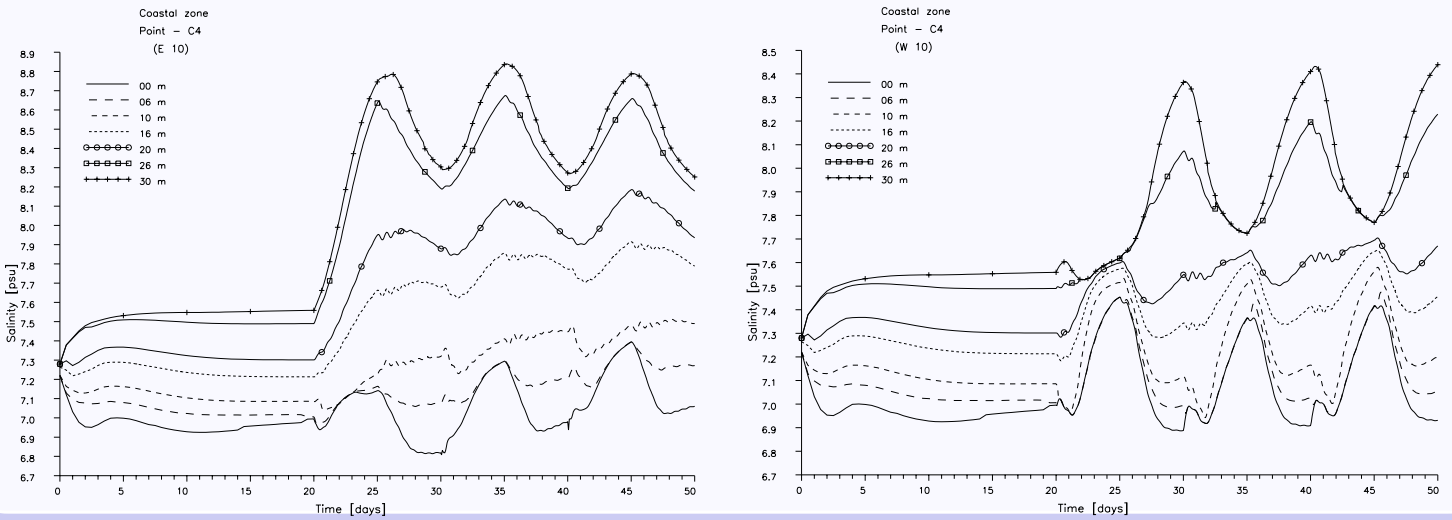

Figure 3 Continued c. point F.

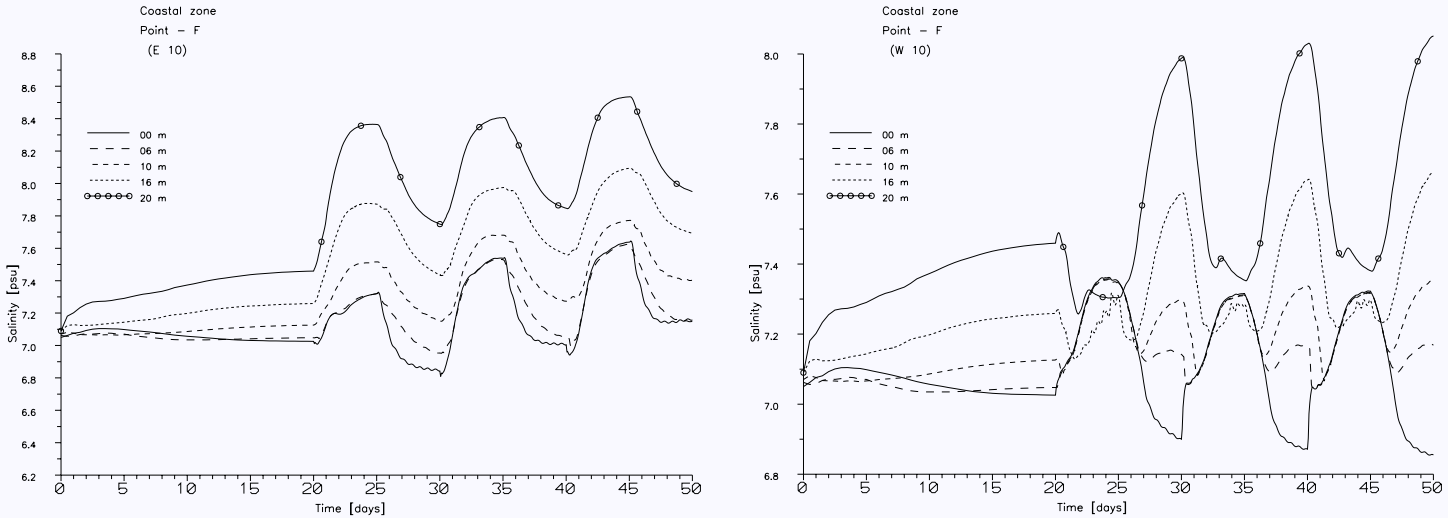

Figure 3 Continued d. point G.

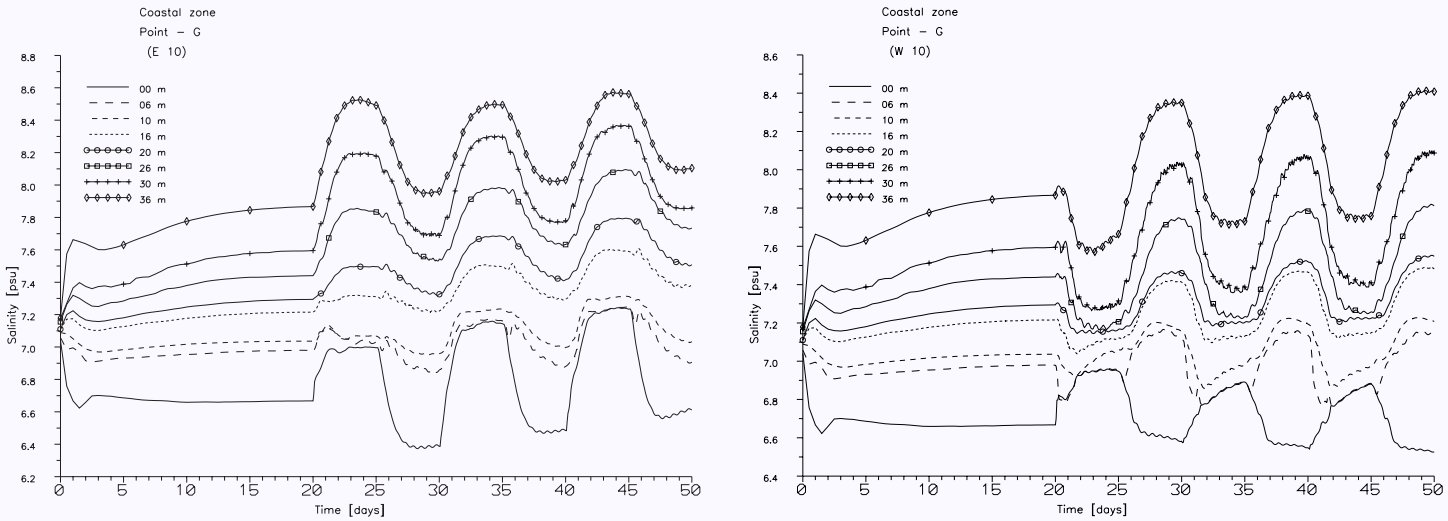

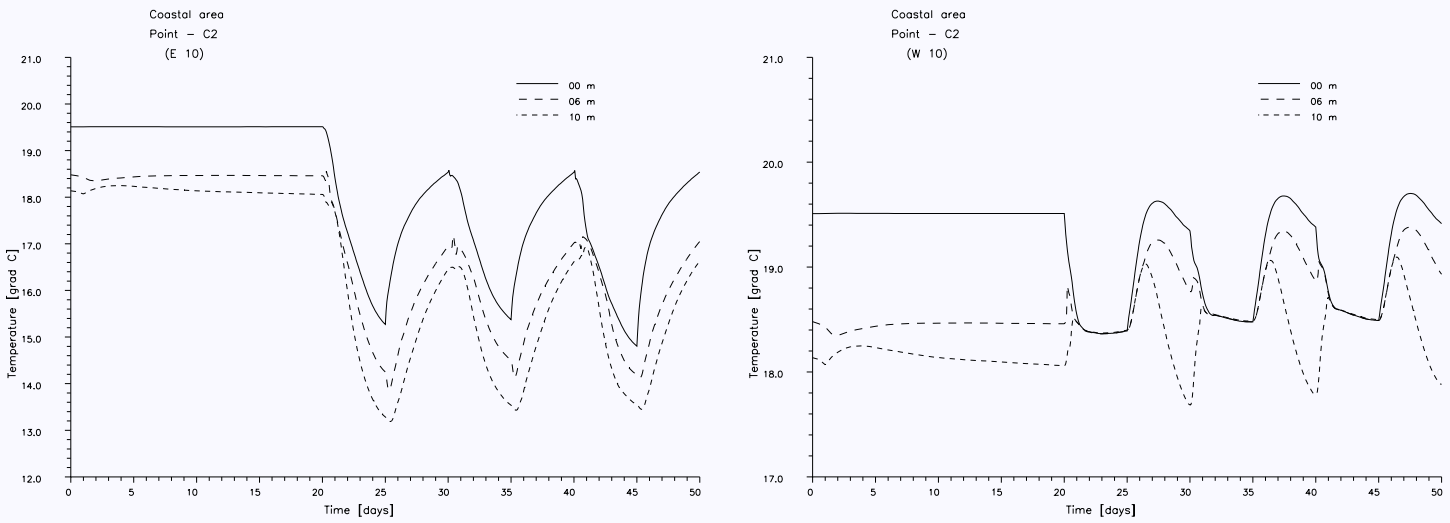

Figure 4: Time evolution of sea water temperature (^oC) at the selected points in the southern Baltic Sea calculated for the case of storms with wind from East (left panel) and from West (right panel). a. point C2. Time course of wind stress is shown in Fig. 1. Location of points – see Fig. 2.

Figure 4 Continued b. point C4.

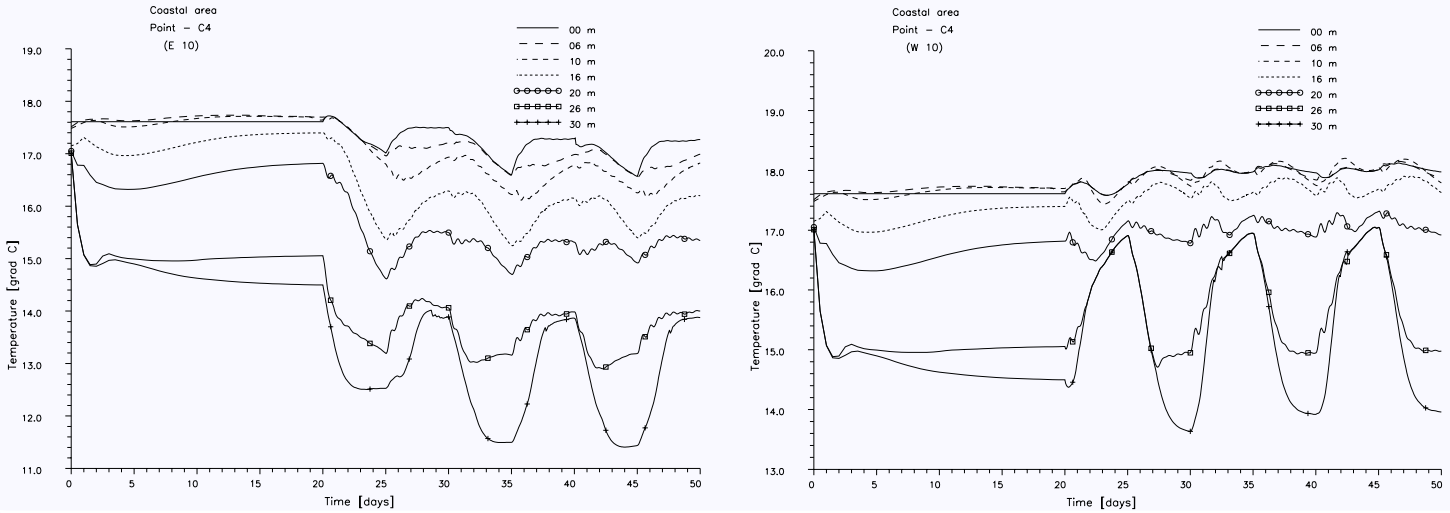

Figure 4 Continued c. point F.

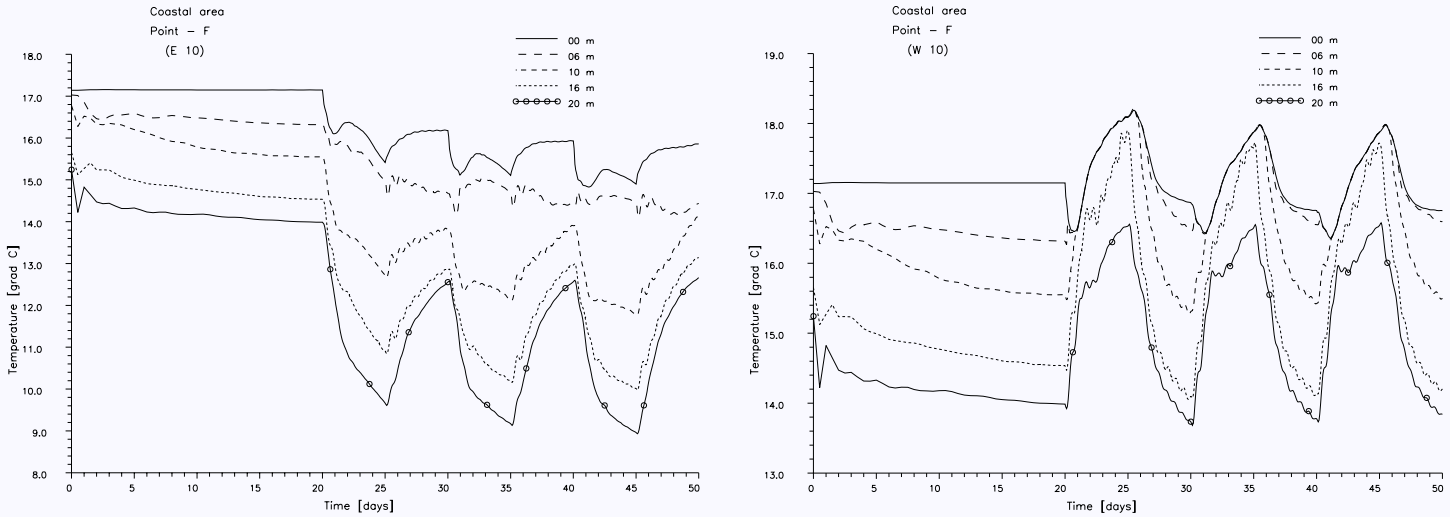

Figure 4 Continued c. point G.

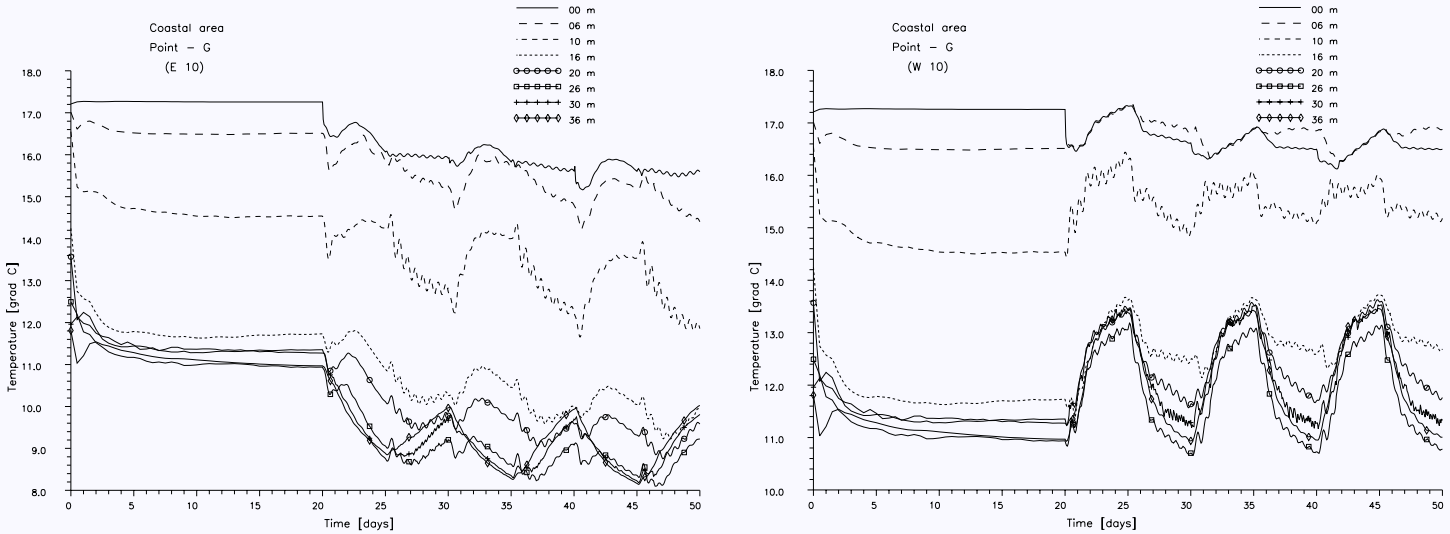

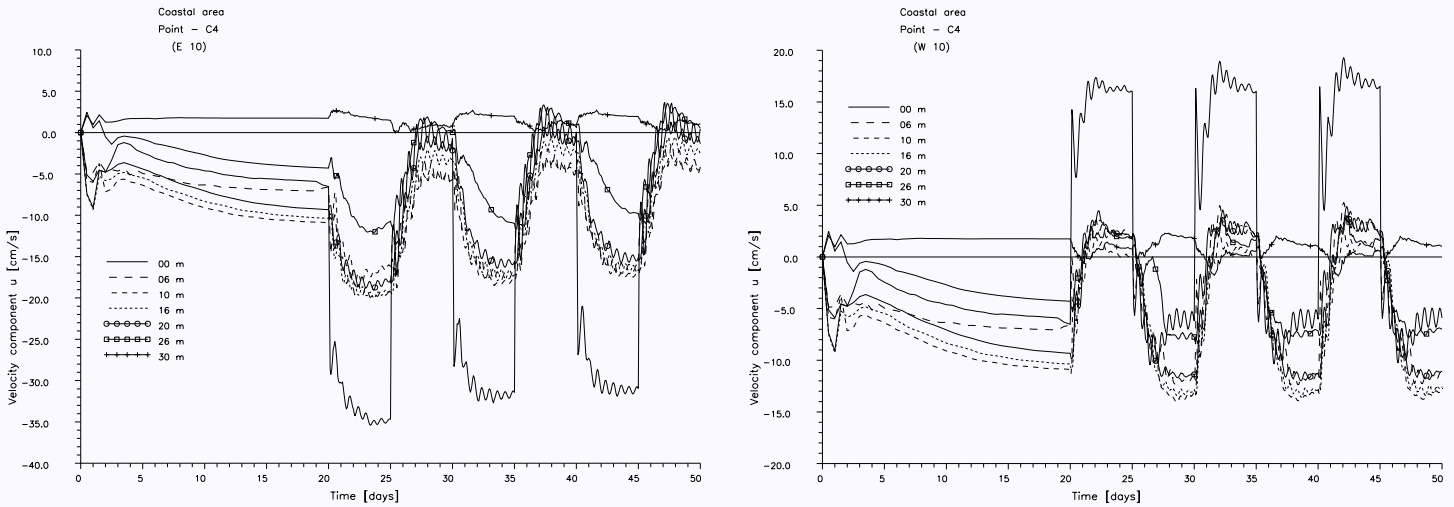

Figure 5: Time evolution of alongshore, zonal current velocity component u (cm/s) at the selected points in the southern Baltic Sea calculated for the case of storms with wind from East (left panel) and from West (right panel). Positive values of velocity indicate alongshore eastwards flow. a. point C4. Time course of wind stress is shown in Fig. 1. Location of points – see Fig. 2.

Figure 5 Continued b. point F.

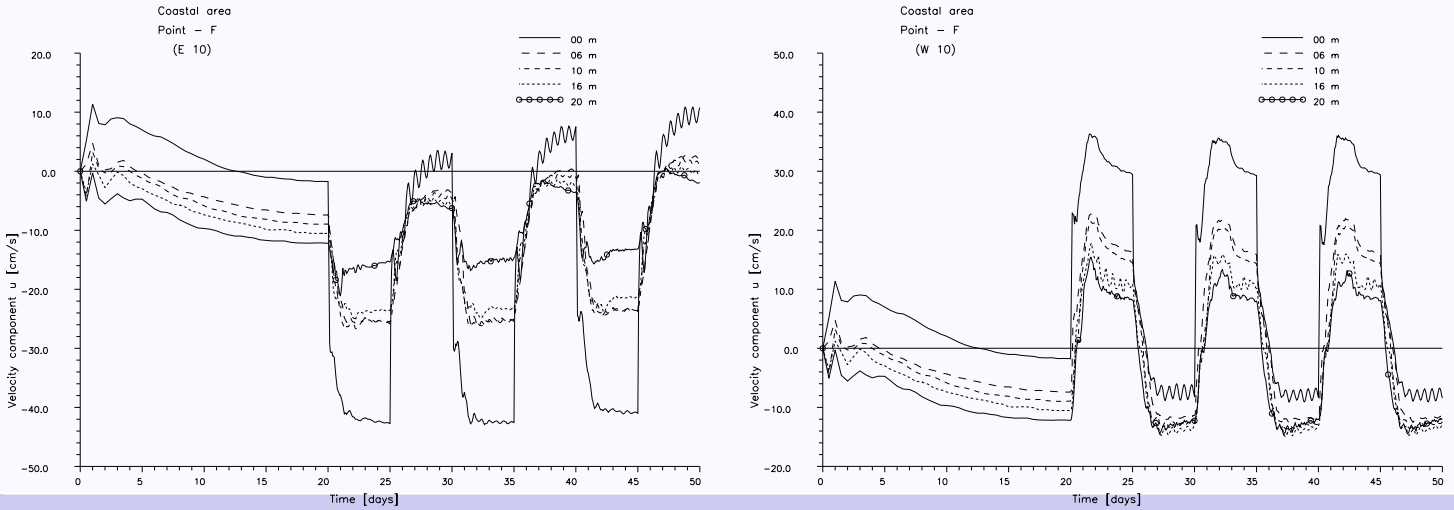

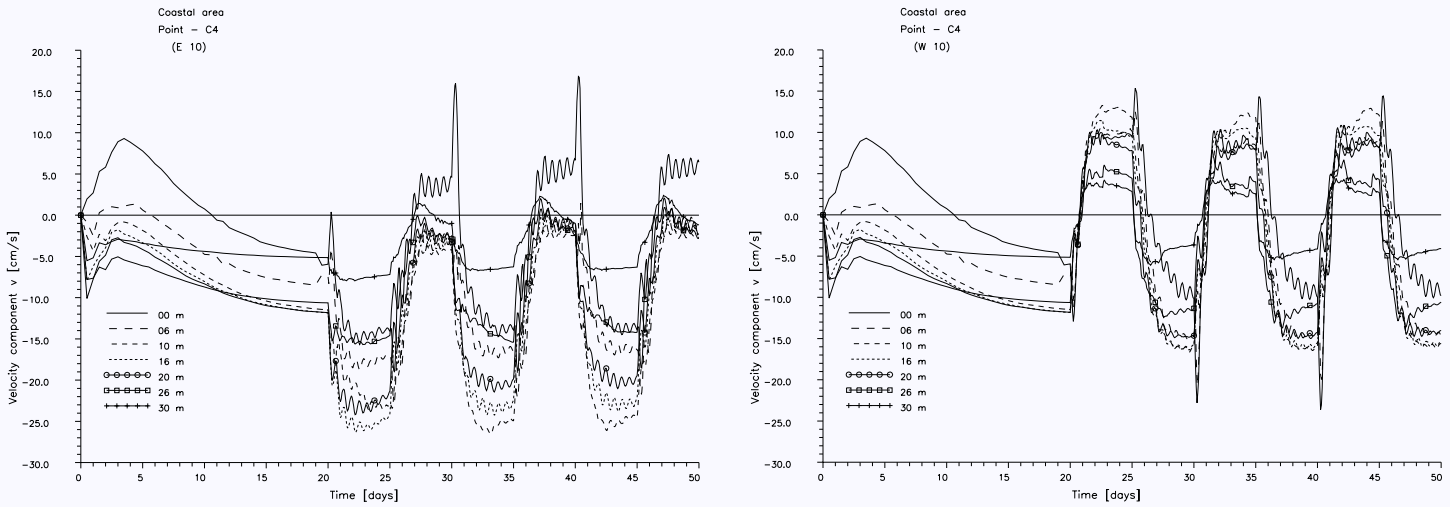

Figure 6: Time evolution of crossshore, meridional current velocity component v (cm/s) at some depths at the selected points in the southern Baltic Sea calculated for the case of storms with wind from East (left panel) and from West (right panel). Positive values of velocity indicate offshore flow, negative - onshore flow. a. point C4. Time course of wind stress is shown in Fig. 1. Location of points – see Fig. 2.

Figure 6 Continued b. point F.

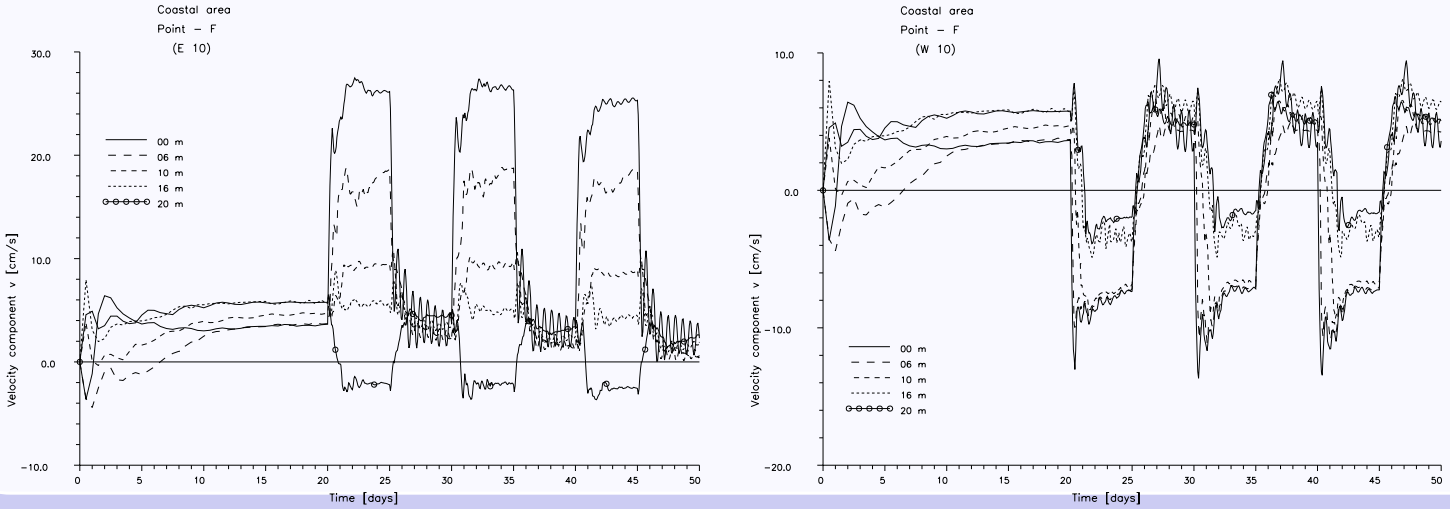

From the above figures it follows that the behaviour of the coastal waters is as it can be expected:

- strong alongshore currents in wind direction of wind;
- intense water exchange in cross shore direction: offshore flow in the upper layers and onshore flow in the bottom layes for the winds from East and in opposite directions in the case the winds from West;
- intensive fluctuations of temperature and salinity at different depths as can be observed during upwelling/downwelling.

As can be seen from Figs. 3 – 6 the principal response of the stratified southern Baltic basin to an onset of constant wind is in general in a good agreement with Ekman's theory and the results of other studies carried out in different basins, both theoretically and as by numerical modelling (cf. e.g. **Bennett, 1974**; **Fennel, 1986**; **Krauss, 1991**).

In next figure (Fig. 7) the charts of sea water temperature at the depth of 5 meters in a time sequence of 1 day for the wind from SE are presented. They demonstrate time history of occurence of coastal upwelling and its evolution during and next its disappearence in next 5 days after storm when wind was shut down.

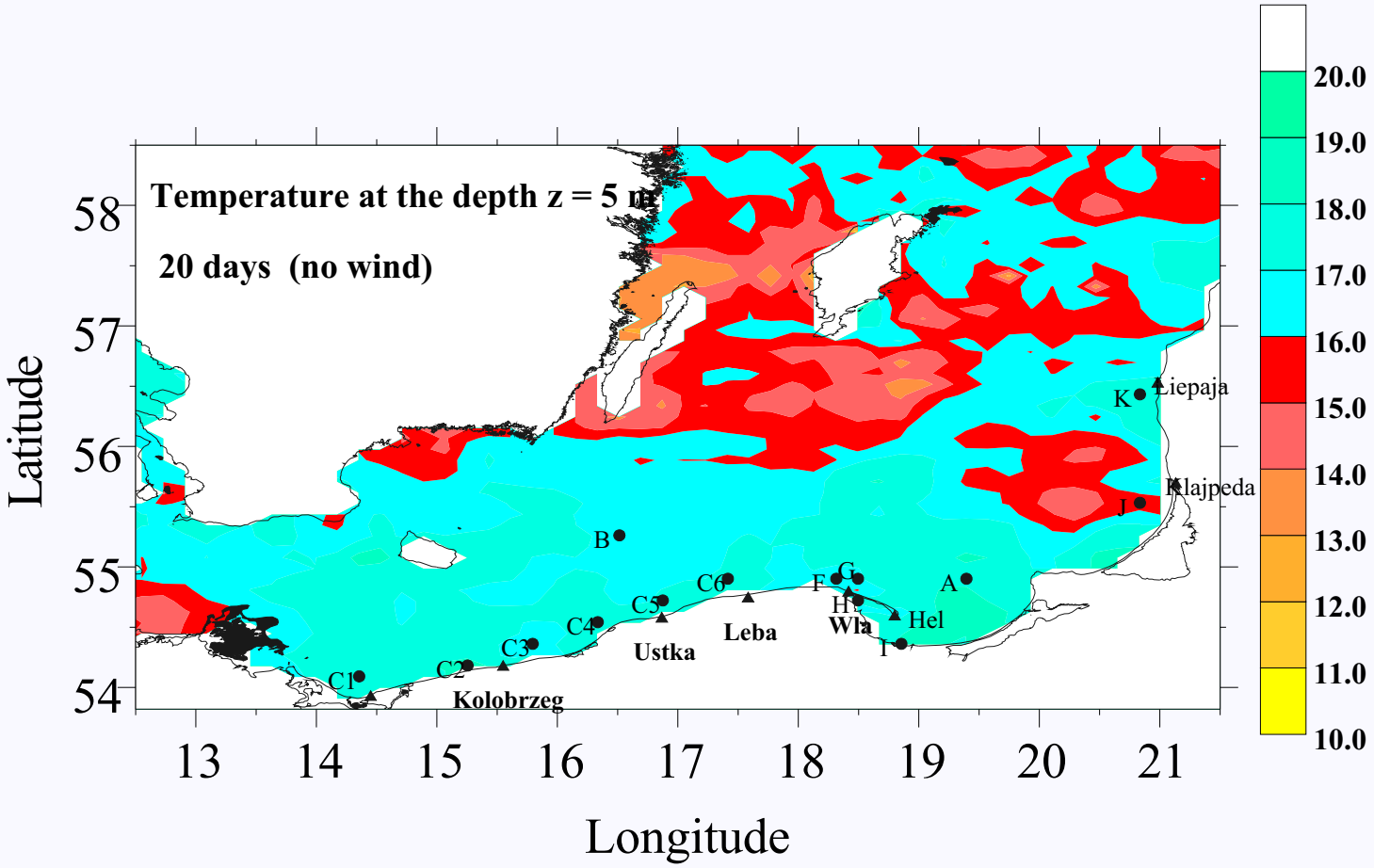

Figure 7: Simulated sea water temperature [^oC] at the depth of 5 meters in a time sequence of 1 day.
a. day 20th – at end of the first stage of calculations during which model was forced only by climatology (without wind). Time course of wind stress is shown in Fig. 1.

Figure 7 Continued b. day 21st – wind from SE.

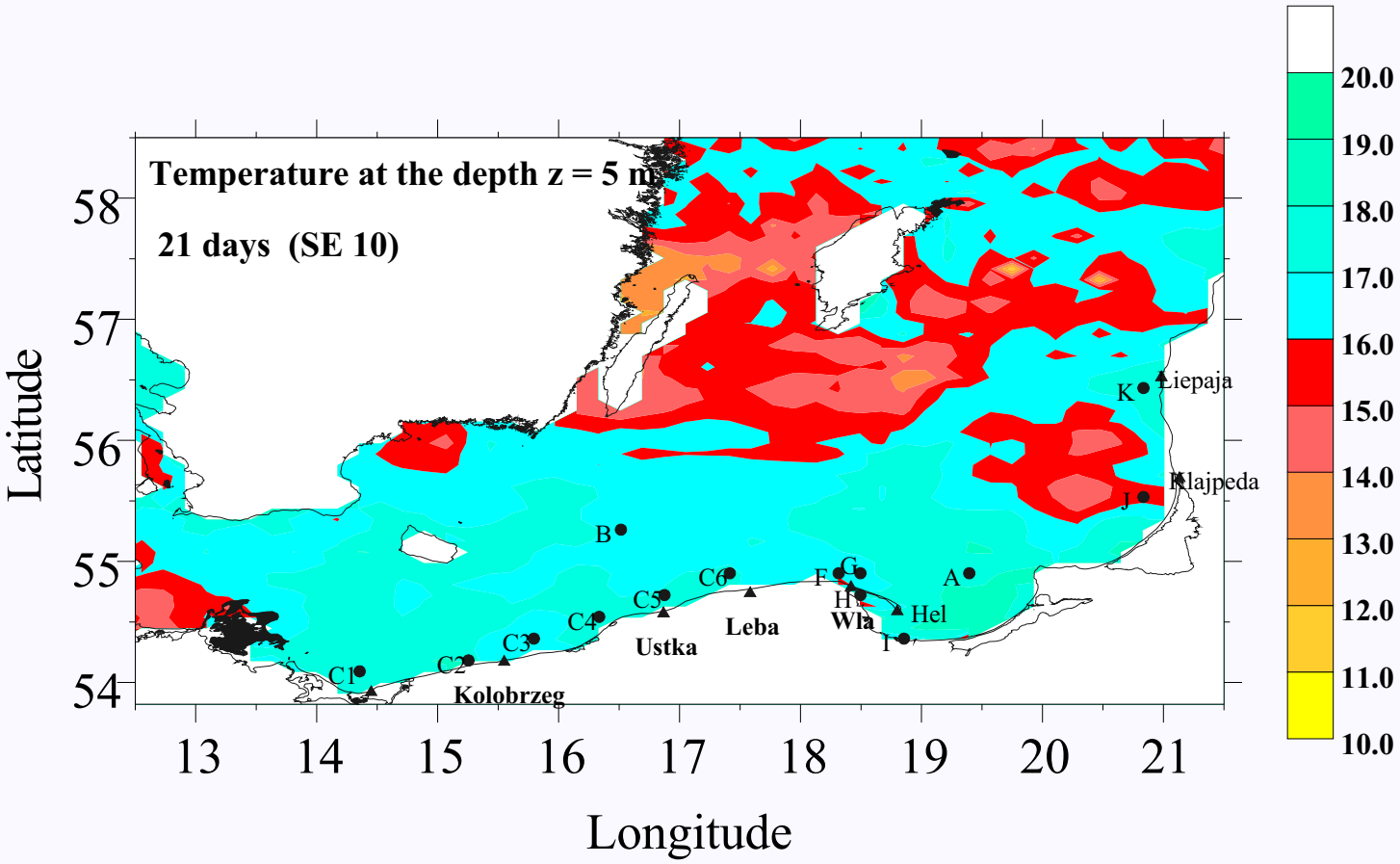

Figure 7 Continued c. day 22nd – wind from SE.

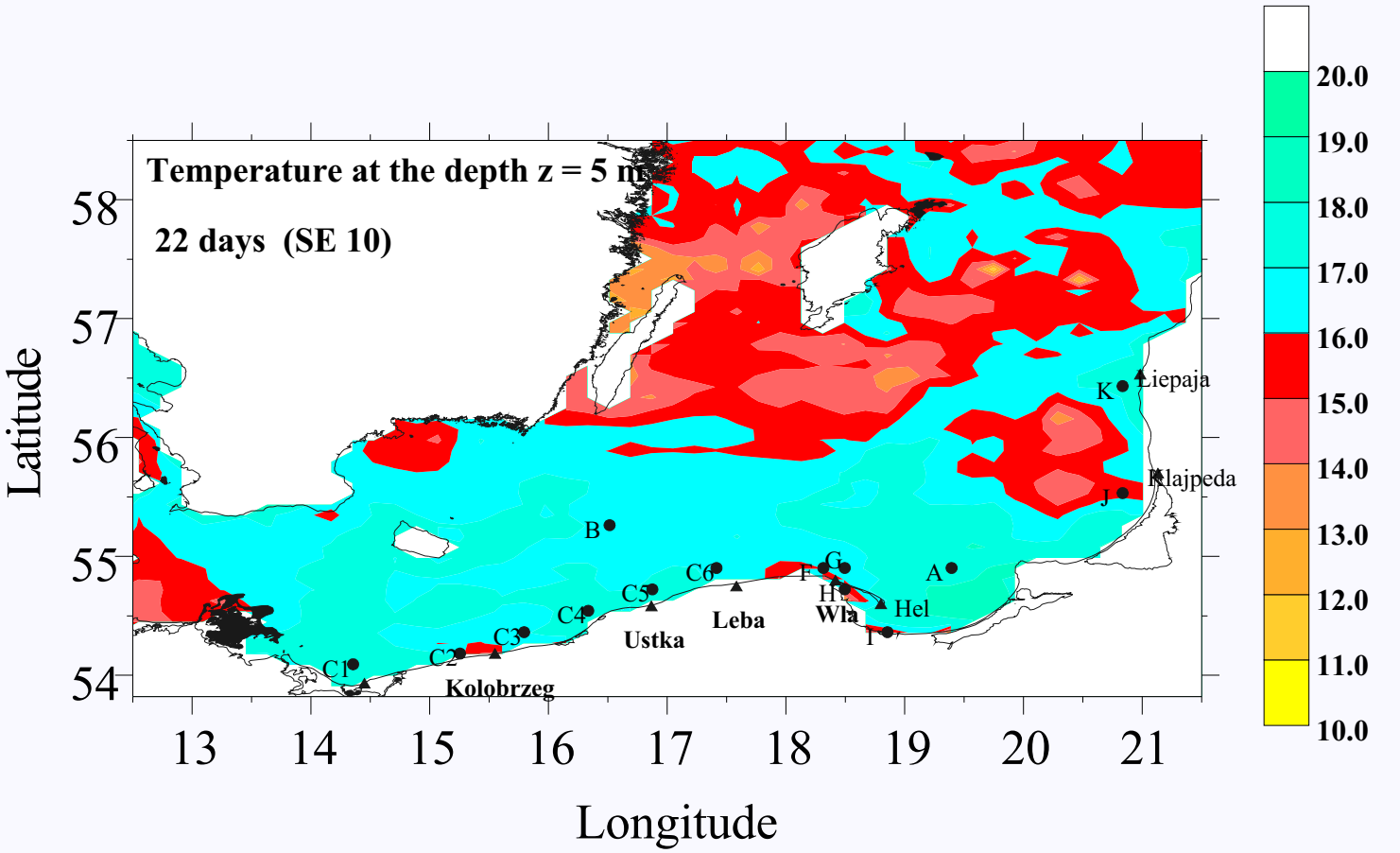

Figure 7 Continued d. day 23rd – wind from SE.

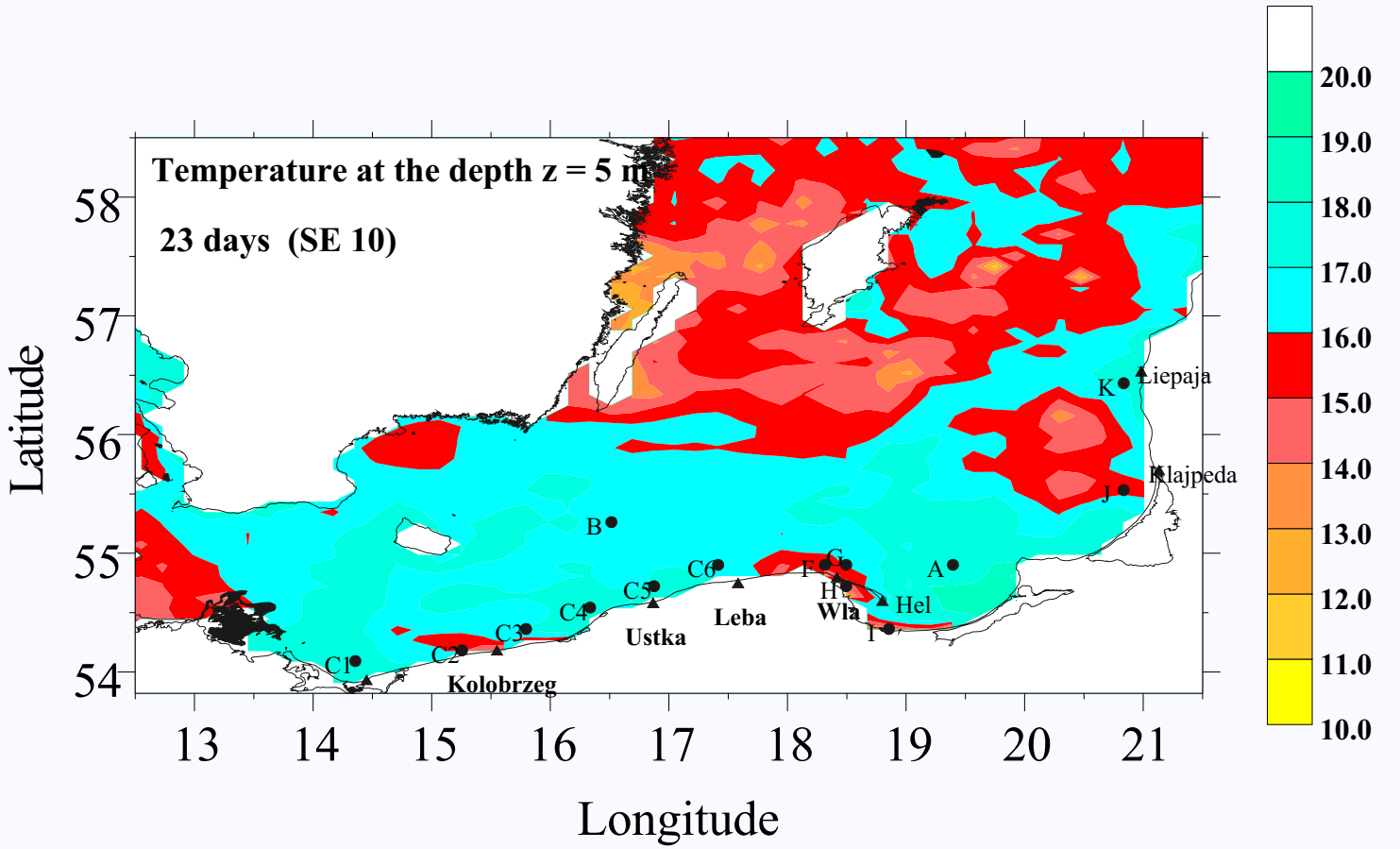

Figure 7 Continued e. day 24th – wind from SE;

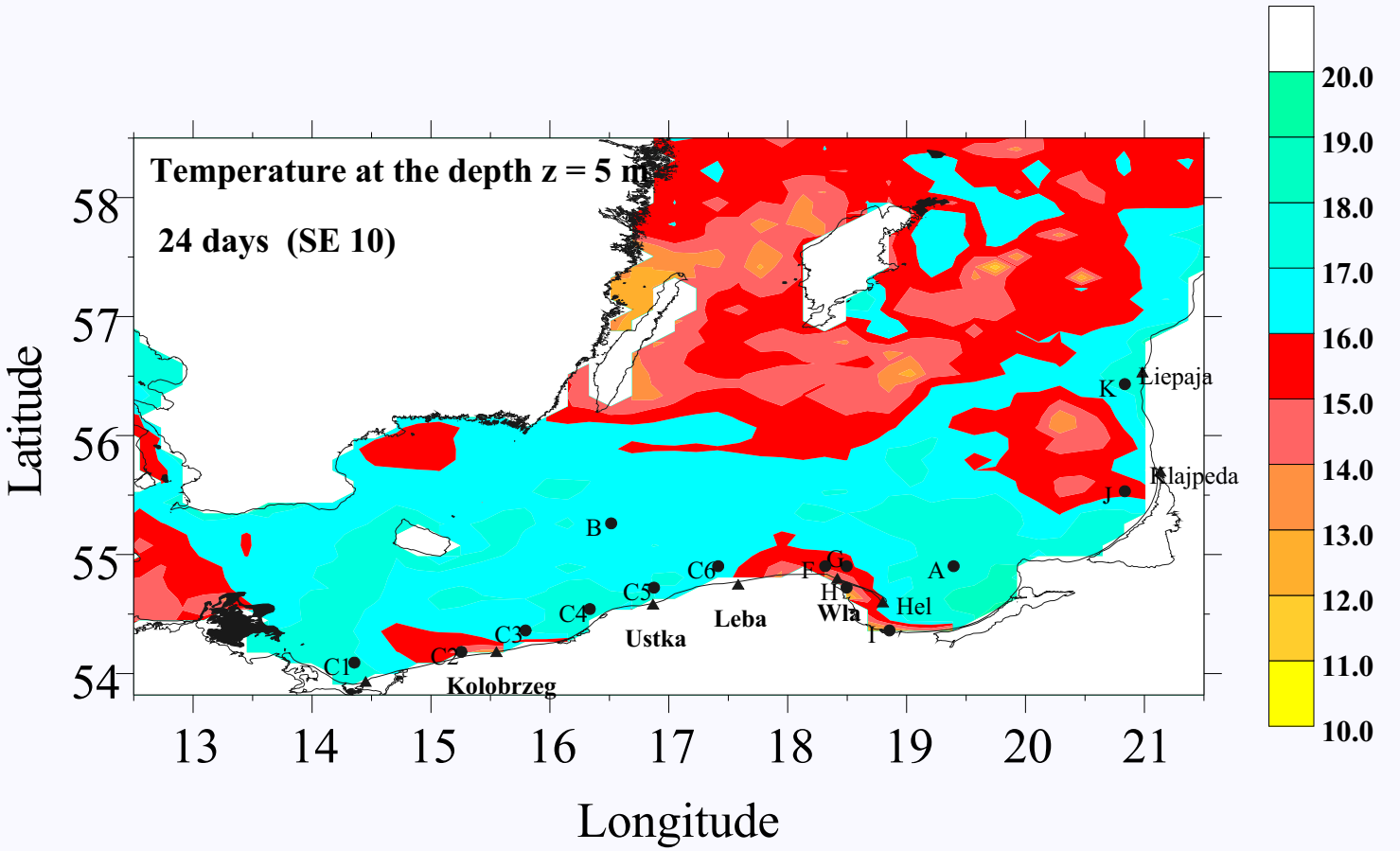

Figure 7 Continued f. day 25th – wind from SE.

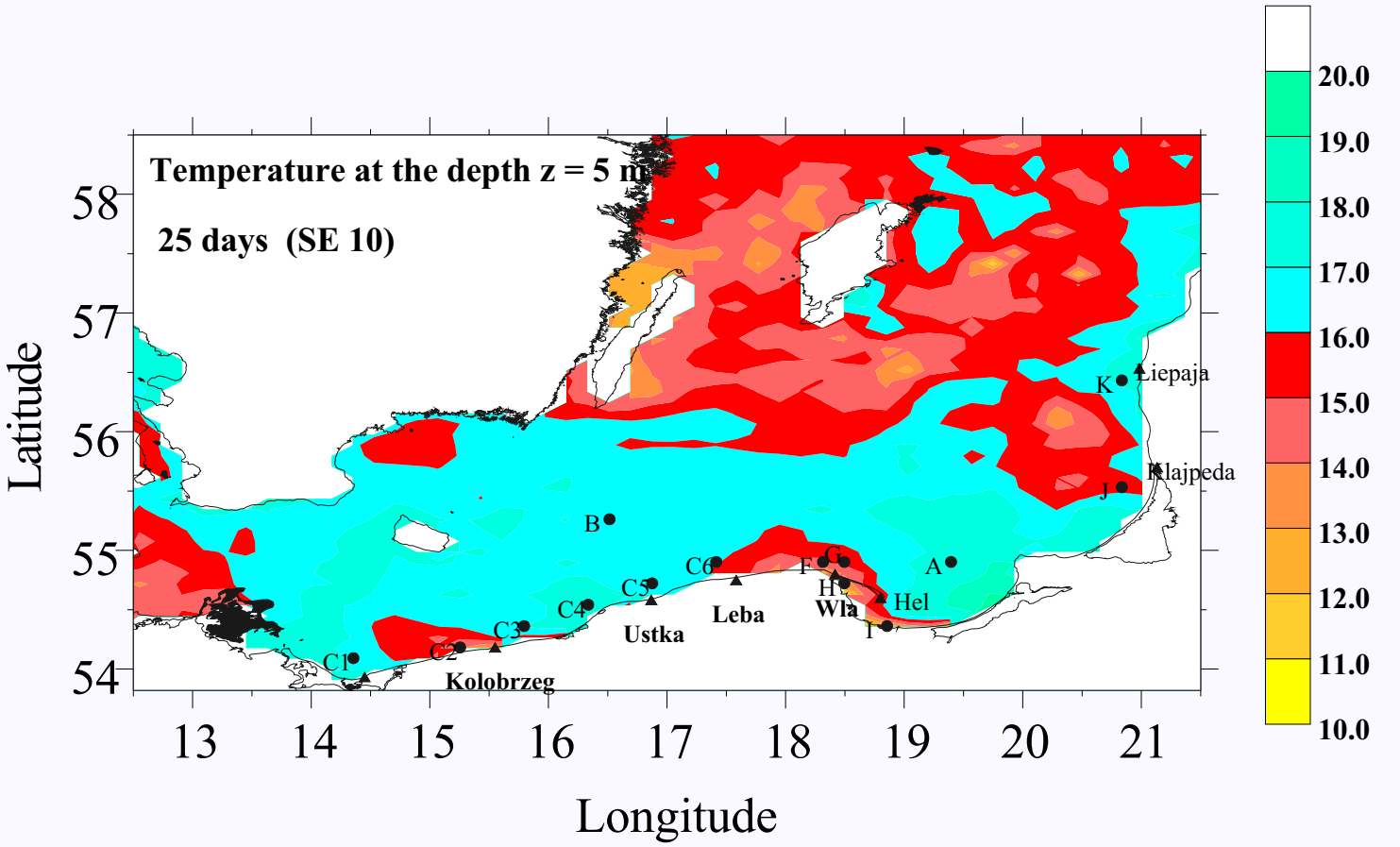

Figure 7 Continued g. day 26th – 1st day after storm with wind from SE.

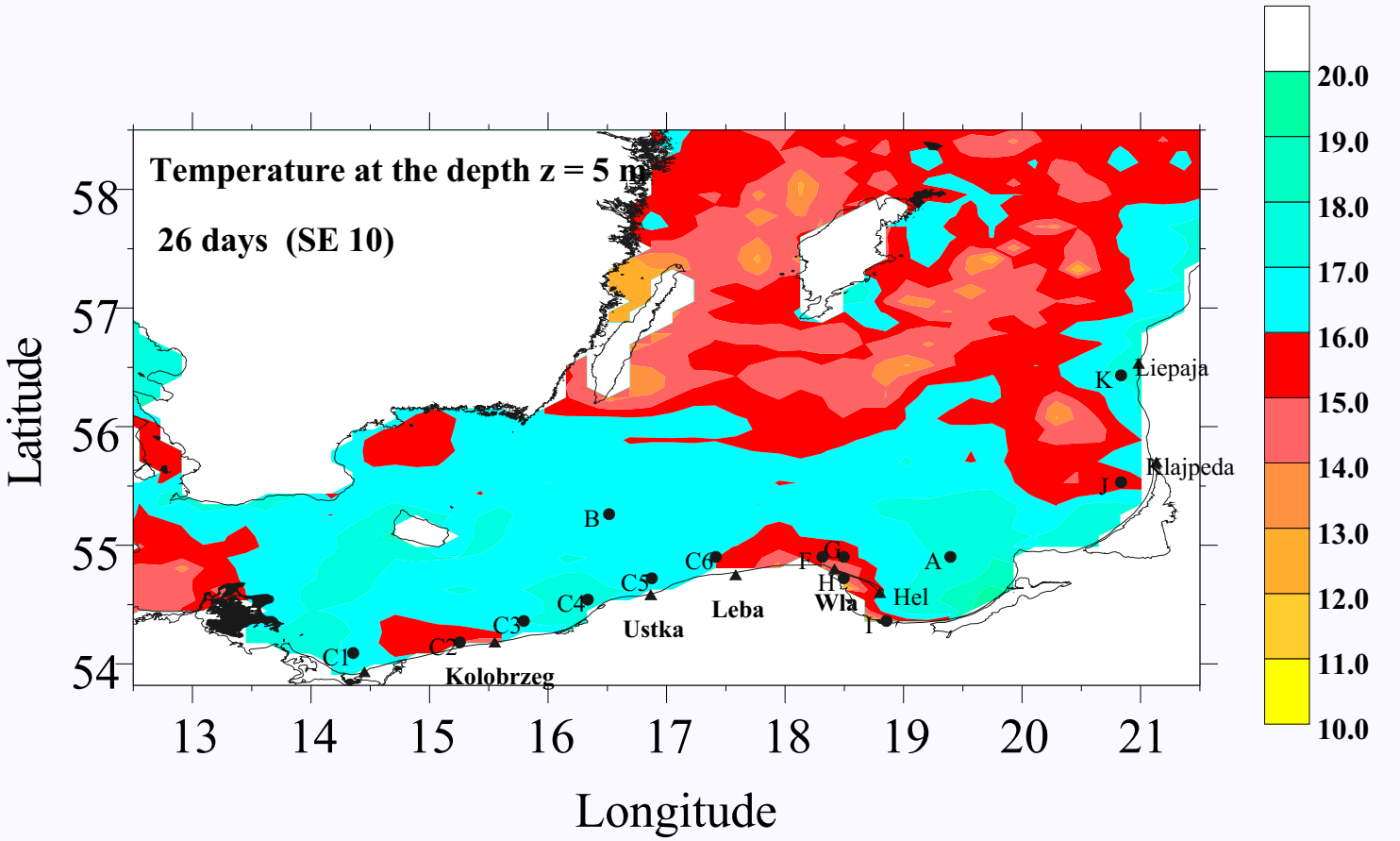

Figure 7 Continued h. day 27th – 2nd day after storm with wind from SE.

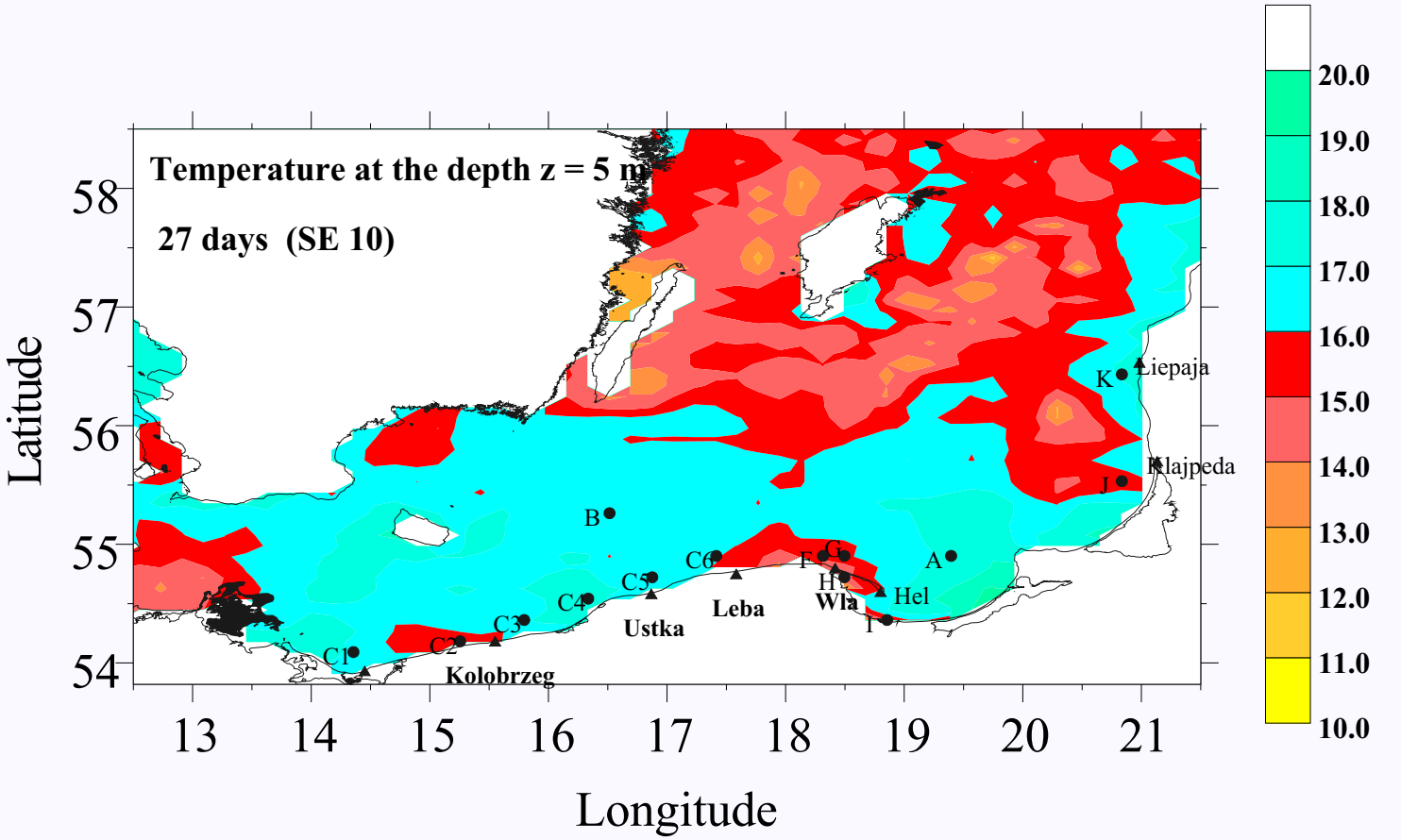

Figure 7 Continued i. day 28th – 3rd day after storm with wind from SE.

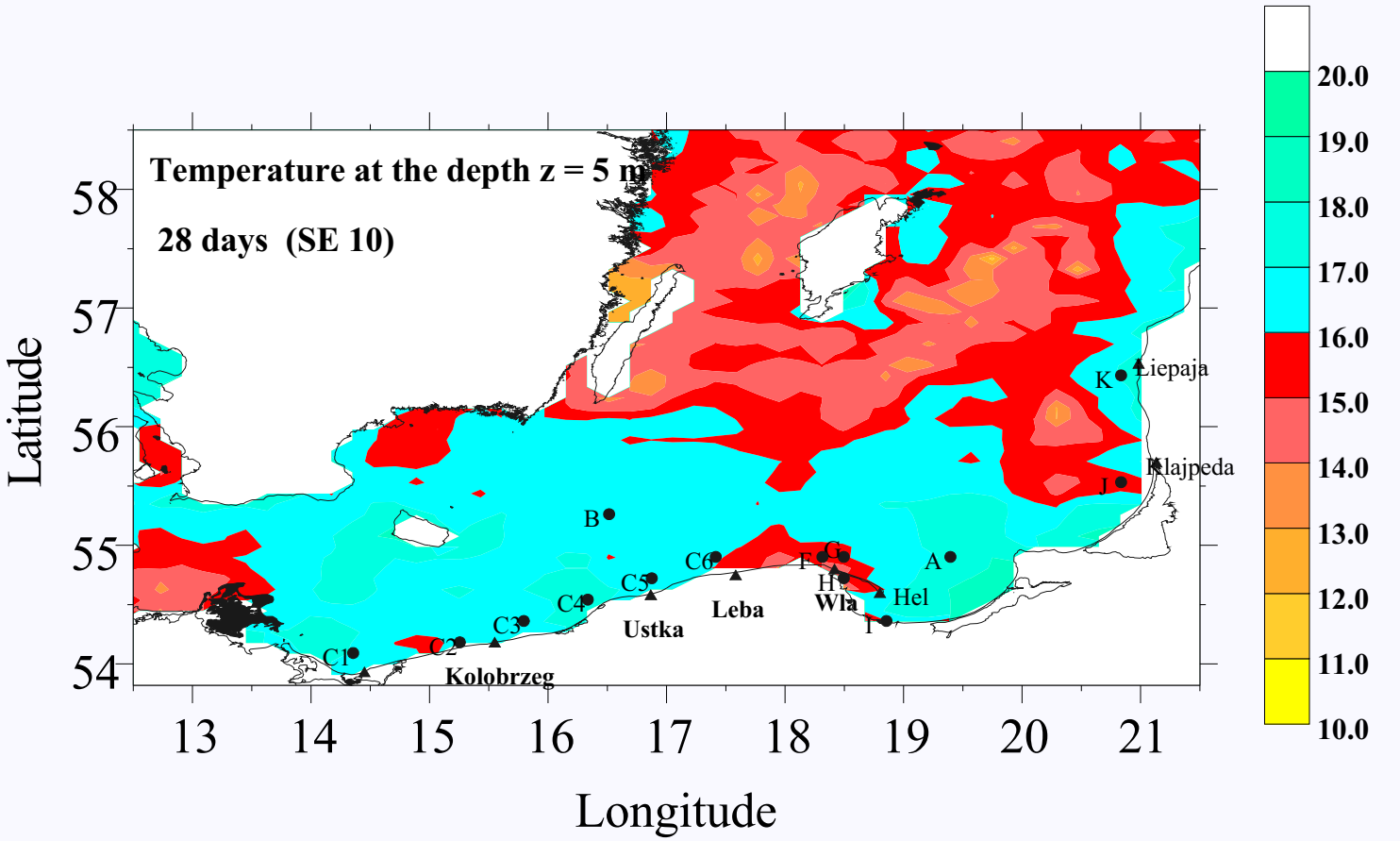

Figure 7 Continued j. day 29th – 4th day after storm with wind from SE.

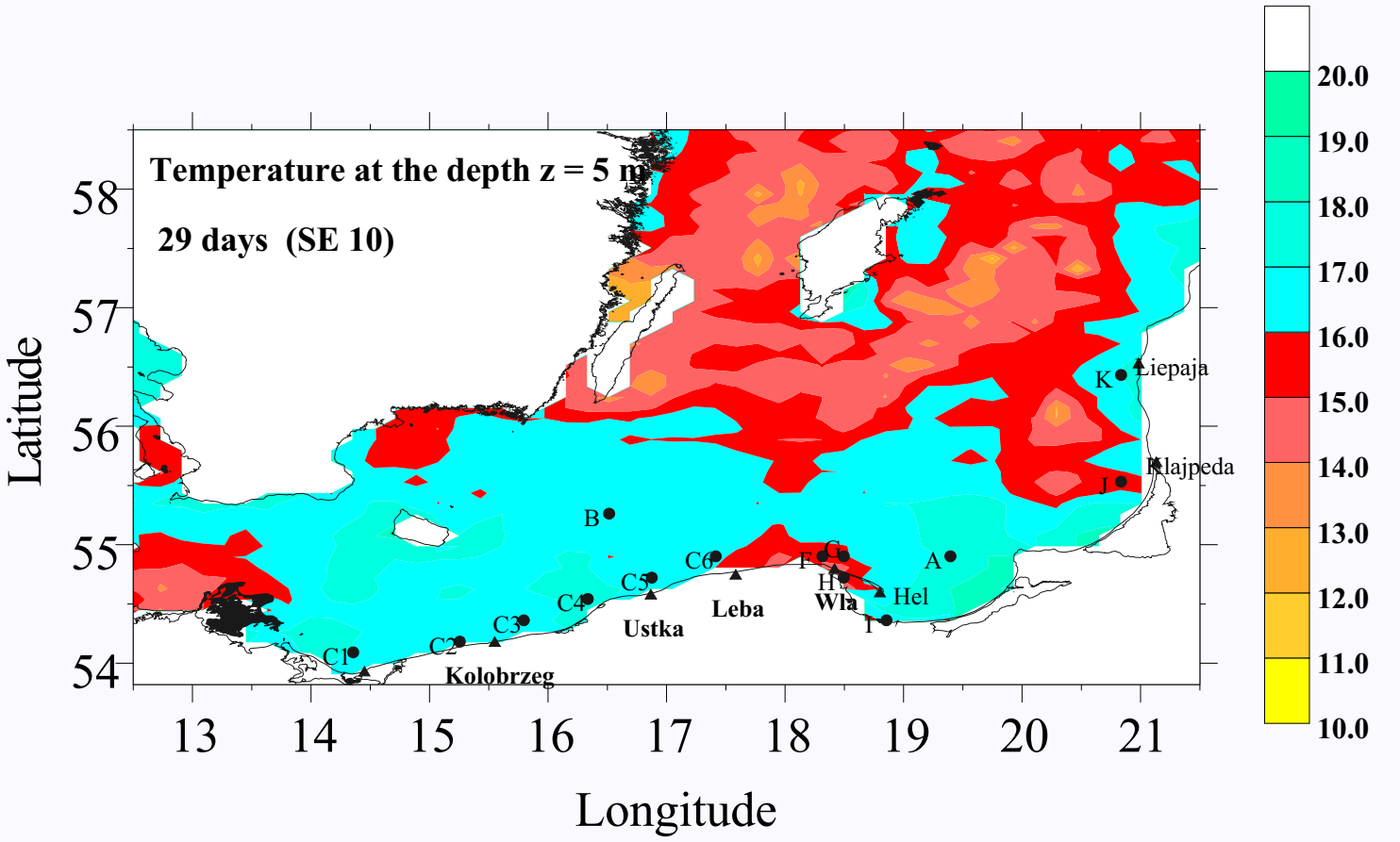

Figure 7 Continued k. day 30th – 5th day after storm with wind from SE.

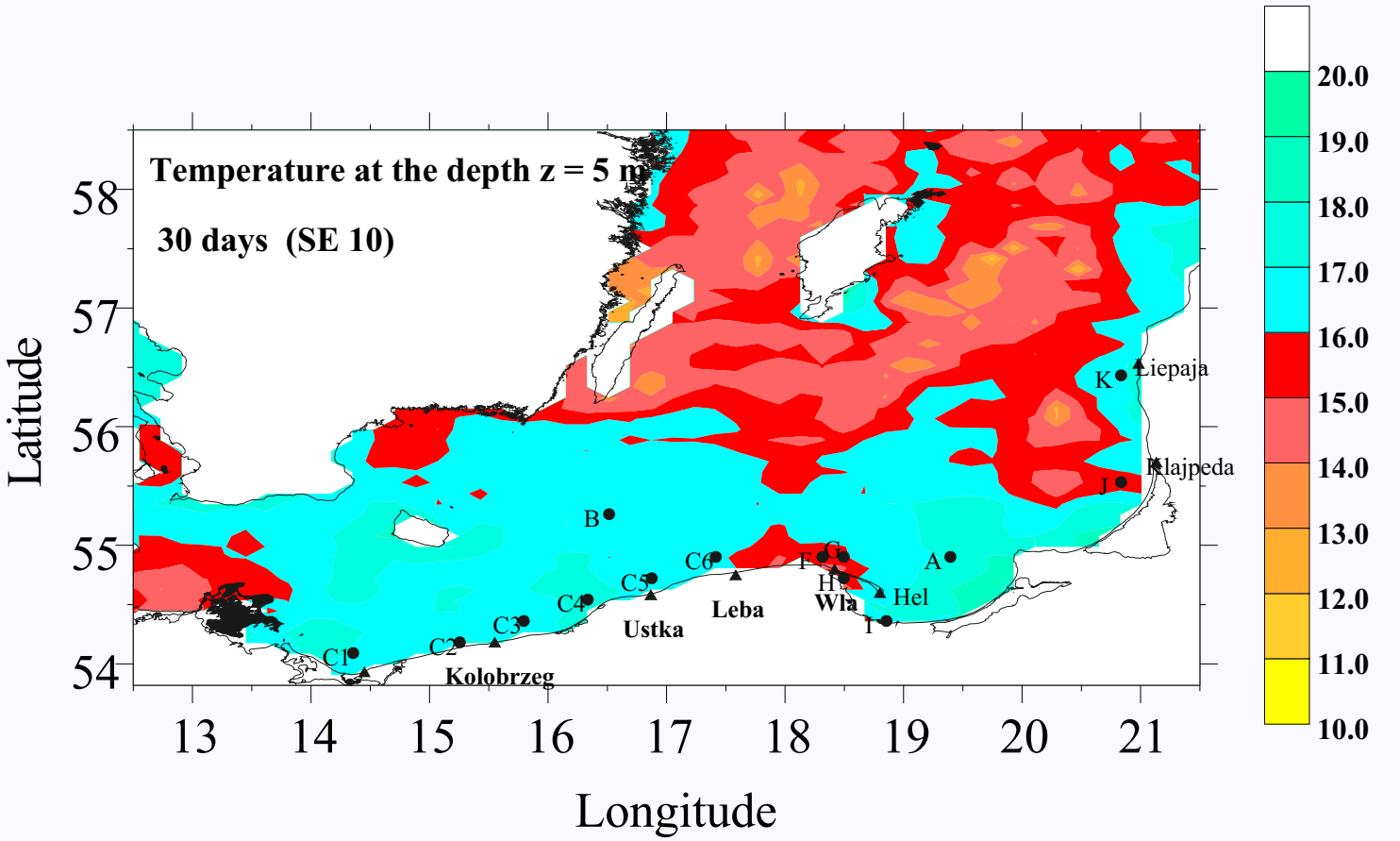

Figure 8 depicts charts of distribution of calculated temperature in surface layer (at the depth of 5 meters) at the end of the first storm i.e., after 25 days of simulation (i.e. at the 5th day of the second stage). The winds blowing from the main 8 directions were considered.

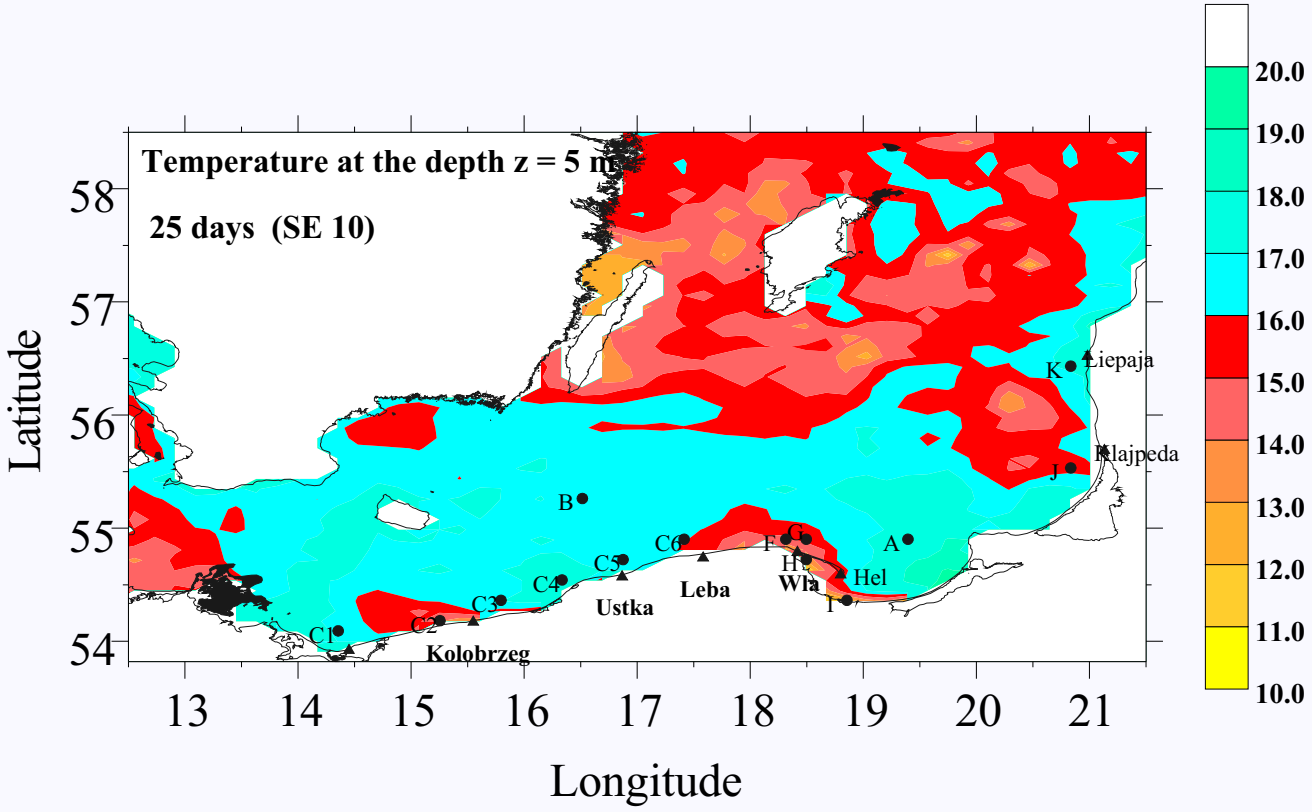

Figure 8: Simulated sea water temperature [^oC] at the depth of 5 meters at the end of the first storm. a. wind from SE. Example of time course of wind stress is shown in Fig. 1.

Figure 8 Continued b. wind from E.

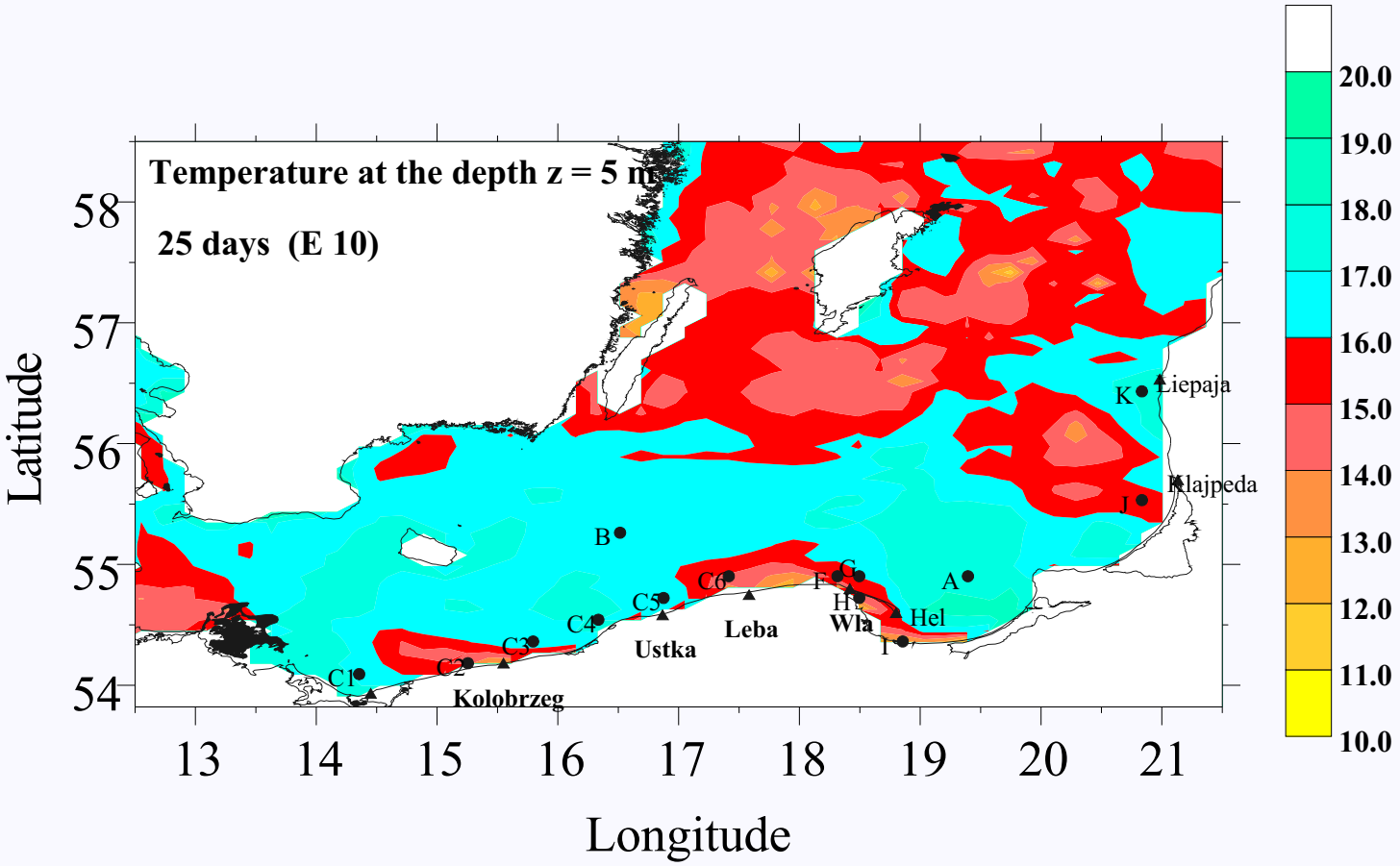

Figure 8 Continued c. wind from NE.

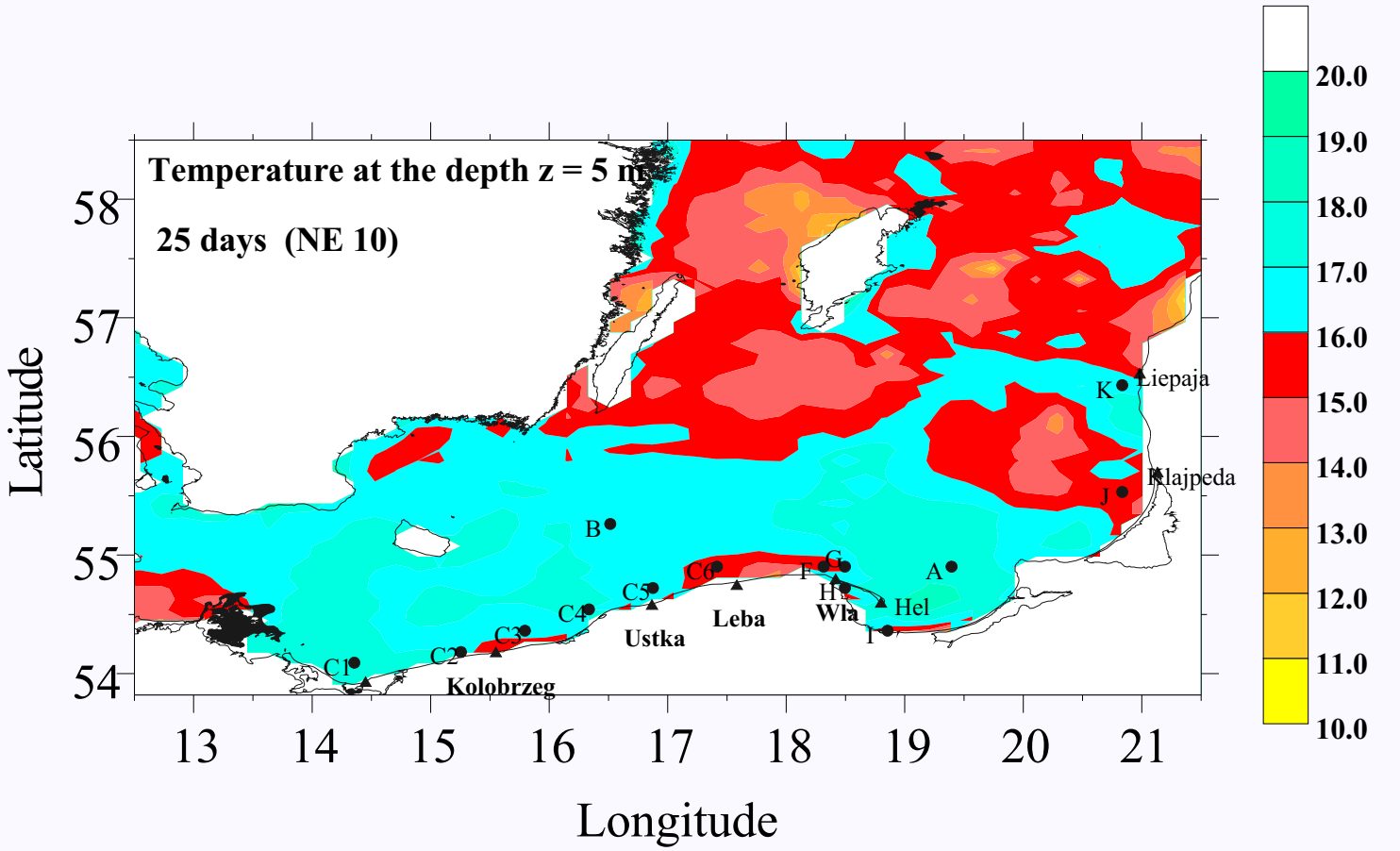

Figure 8 Continued d. wind from N.

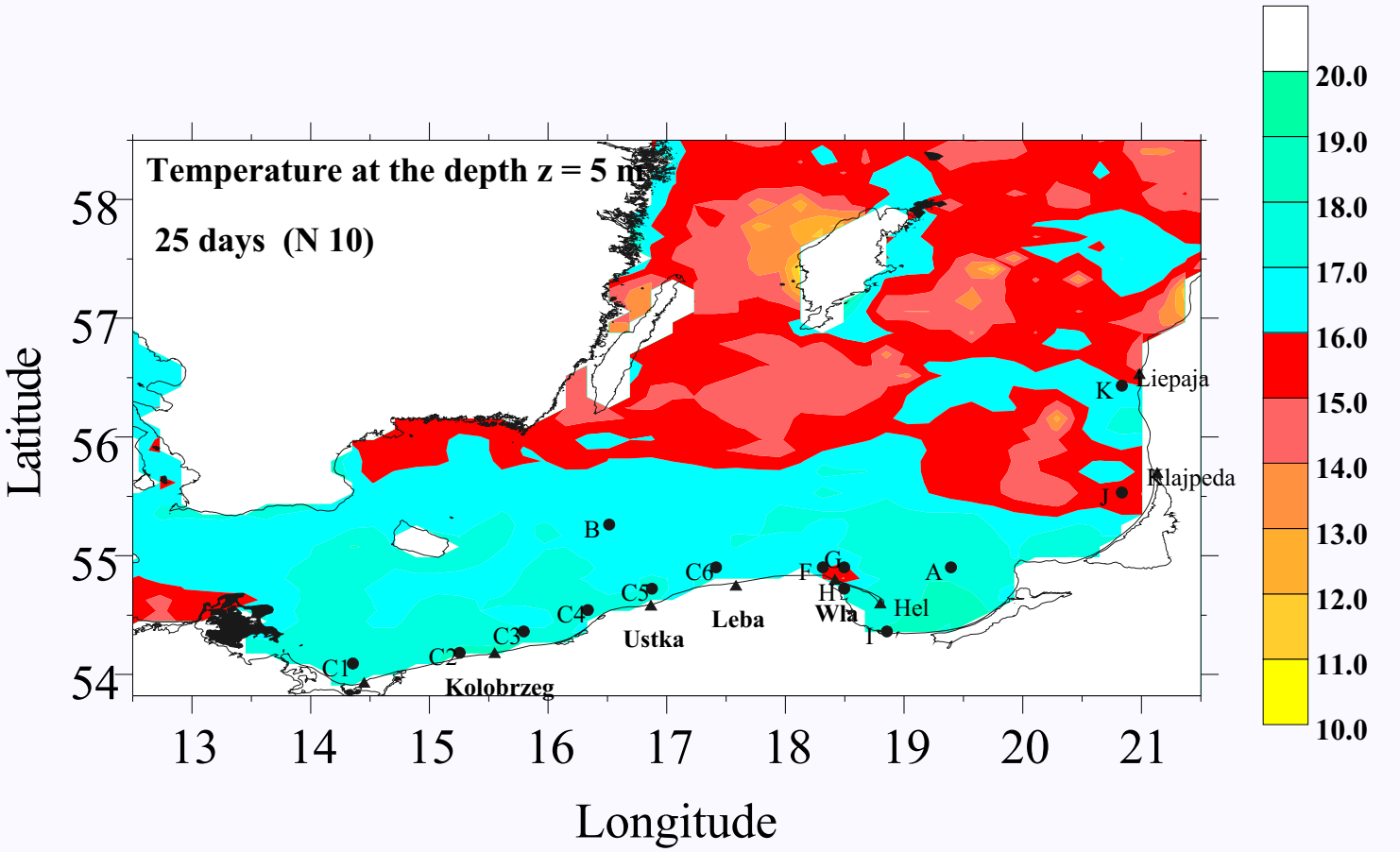

Figure 8 Continued e. wind from NW.

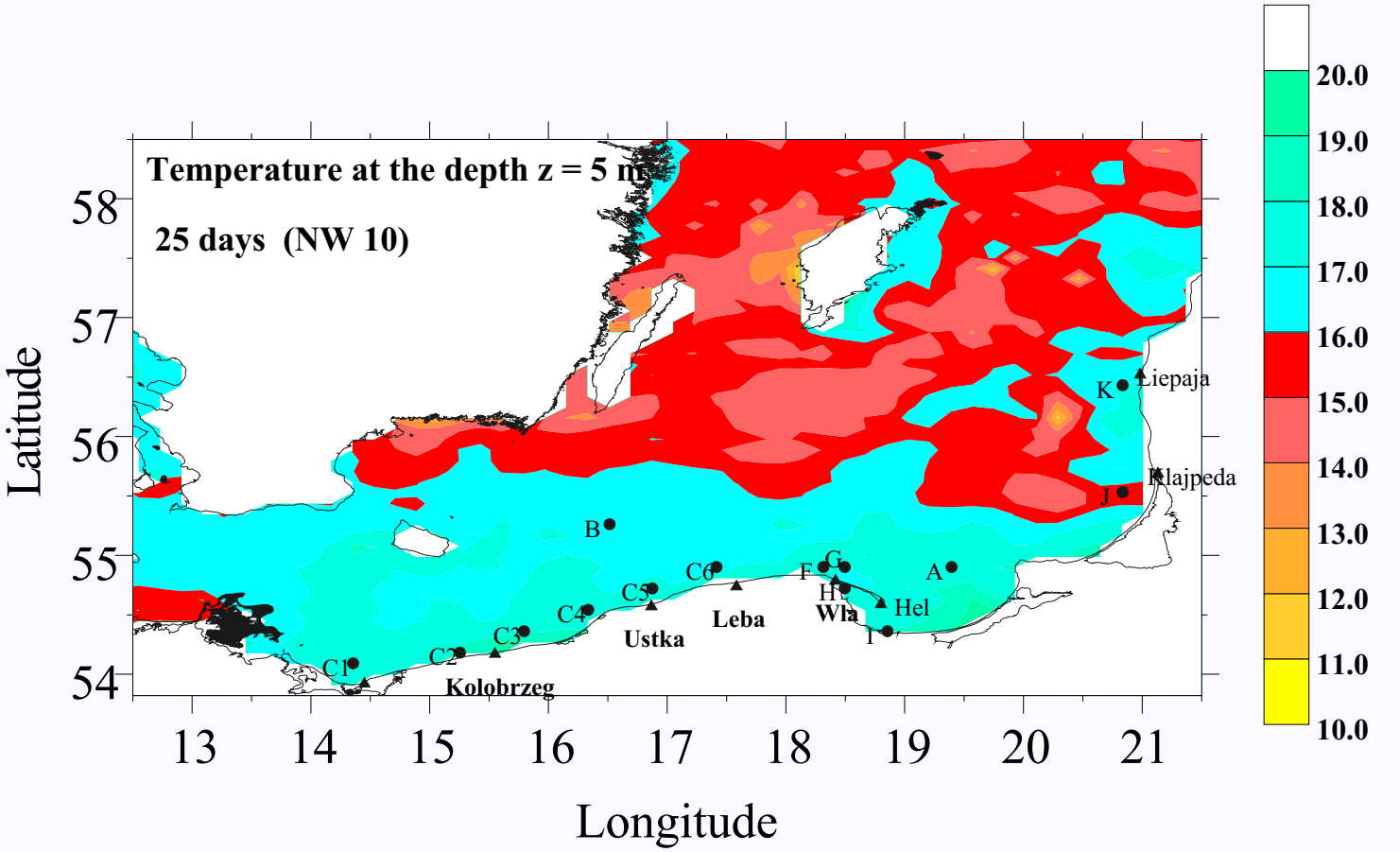

Figure 8 Continued f. wind from W.

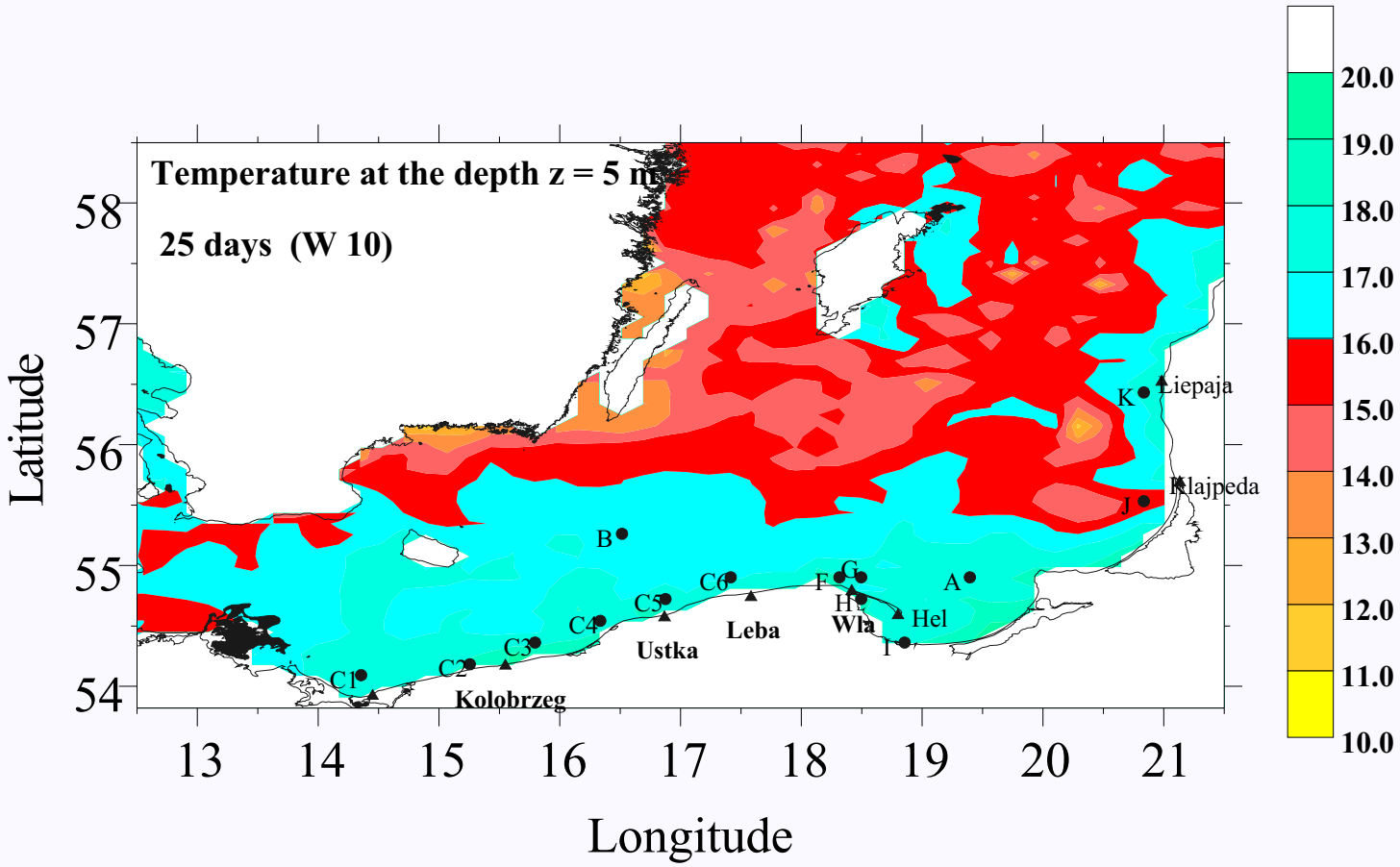

Figure 8 Continued g. wind from SW.

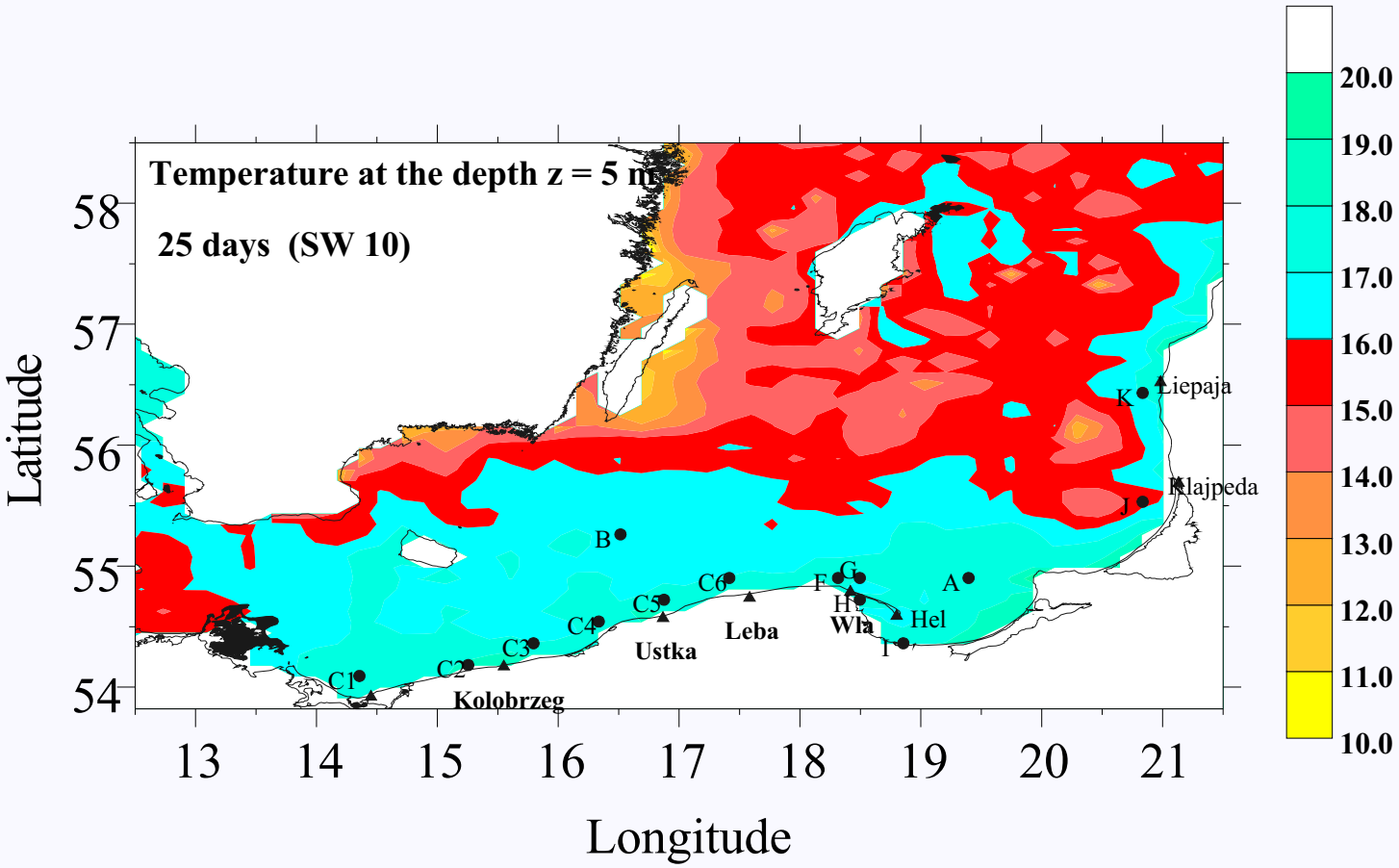

Figure 8 Continued h. wind from S.

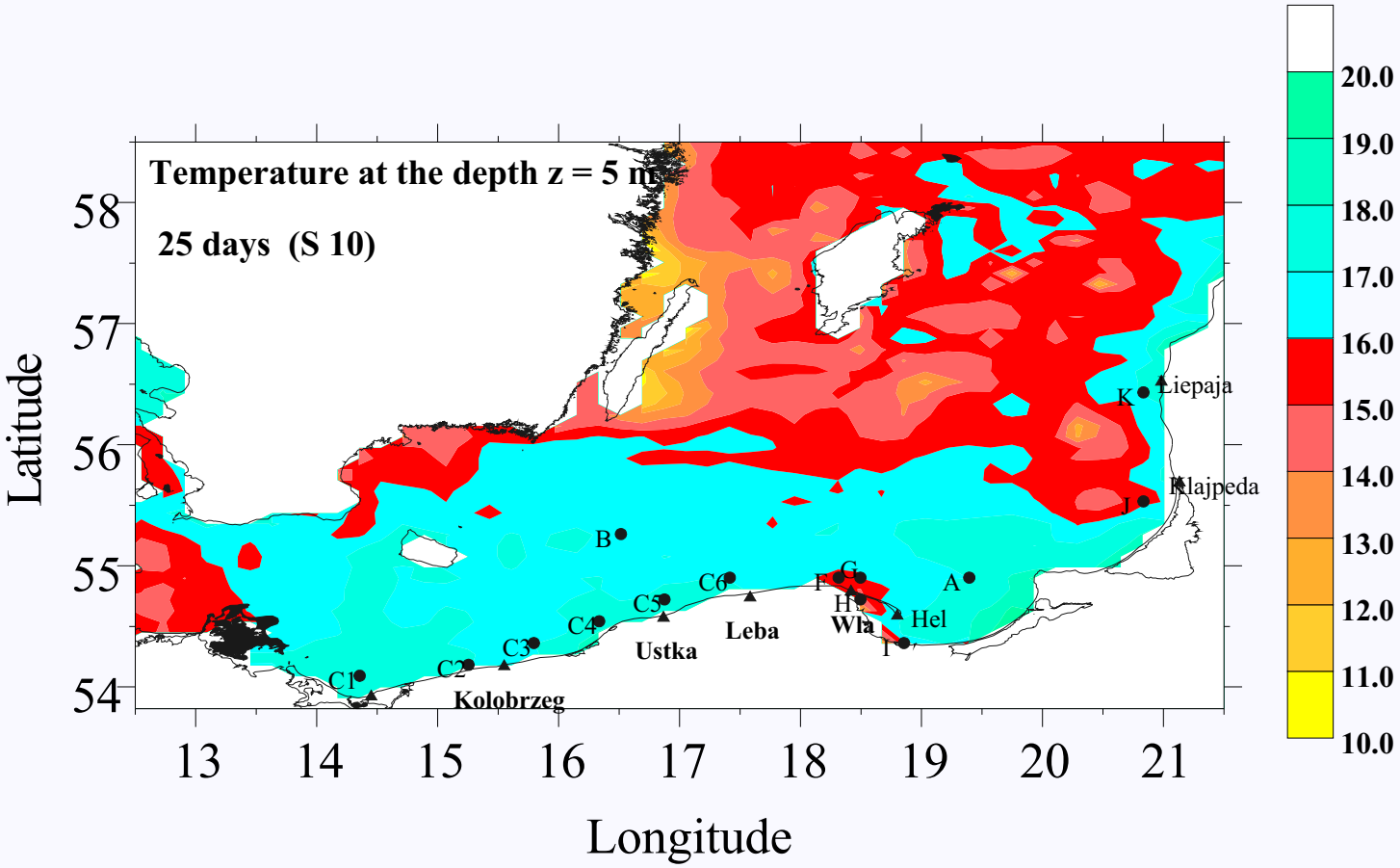

From the above figure it can easily be deduced that the winds from E, NE and SE form the favorable conditions for upwelling at the Polish Baltic coasts. The winds from W, NW and SW are suitable to occur downwelling in that area.

5. CONCLUSIONS

The numerical experiments described here indicate that the POM model is capable of representing the physical processes responsible for the three-dimensional behavior of the coastal area of the southern Baltic.

To demonstrate the utility of the POM code for the Baltic Sea conditions, it was applied to a coastal upwelling situation formed under model forcings of three successive storms of constant wind speed. It appears from the calculations that the model yields results share many features in common with known from studies carried out in the Baltic and in other basins, so theoretically as by numerical models (cf. e.g., **Bennett, 1974**; **Fennel, 1986**; **Krauss, 1991**).

In particular, the results showed that during the winds blowing from E, NE and SE the favorable conditions for upwelling can be observed at the Polish Baltic coasts. The winds from W, NW and SW are suitable to occur downwelling there. These conclusions are in good agreement with results of *in situ* and the satelitte observations (cf. **Bychkova and Viktorov, 1987**; **Bychkova et al., 1988**; **Urbański, 1995**; **Hansen et al., 1993**; **Siegel et al., 1994**).

Acknowledgments This research was supported by grant No. **6 PO4E 020 15** from the Polish State Commitee for Scientific Research.

6. BIBLIOGRAPHY

Bennett, J.R., 1974, *On the dynamic of wind-driven lake currents*, J. Phys. Oceanogr., **4**, 400-414.

Blumberg, A.F., and G. L. Mellor, 1987, *A description of a three-dimensional coastal ocean circulation model*, In: Heaps, N.S., (ed.), *Three-dimensional coastal ocean models*, Coastal and Estuarine Sciences 4, American Geophysical Union, Washington, D.C., 1-16.

Bock, K.H., 1971, *Monatskarten des Salzgehaltes der Ostsee, dargestellt fuer verschiedene Tiefenhorizonte*, Dt. Hydrogr. Z., Erg.-H.R.B., **12**, Hamburg, 148 pp.

Bychkova, I.A., S.V. Viktorov, and D.A. Shumakher, 1988, *A relationship between the large-scale atmospheric circulation and the origin of coastal upwelling in the Baltic Sea*, Meteorologiya i gidrologiya, **10**, 91-98, (in Russian).

Bychkova, I.A., and S.V. Viktorov, 1987, *Elucidation and systematization of upwelling zones in the Baltic Sea based on satellite data*, Okieanologiya, **XXVII**, 218-223, (in Russian).

Elken, J., 1996, *Deep water overflow, circulation and vertical exchange in the Baltic Proper*, Estonian Marine Institute Report Series, **No. 6**, Tallinn, 91 pp.

Ezer, T.L., and G. L. Mellor, 1994, *Diagnostic and prognostic calculations of the North Atlantic circulation and sea level using a sigma coordinate ocean model*, J. Geophys. Res., **99(C7)**, 14159-14171.

Ezer, T.L„ and G.L. Mellor, 1997, *Simulations of the Atlantic Ocean with a free surface sigma coordinate ocean model*, J. Geophys. Res., **102 (C7)**, 15647-15657.

Fennel, W., 1986, *On the dynamics of coastal jet*, Rapp. P.-v. Réun. Cons. Int. Explor. Mer., **186**, 31-37.

Gidhagen, L., 1984, *Coastal upwelling in the Baltic Sea*, Proc. 14th Conf. Baltic Oceanographers, Gdynia, vol. 1, 182-190.

Hansen, L., N.K. Hojerslev, and H. Soogaard, 1993, *Temperature monitoring of the Danish marine environment and the Baltic Sea*, Kobenhavns Universitet, Report **52**, 77.

Haapala, J., 1994, *Upwelling and its influence on nutrient concentration in the coastal Area of the Hanko Penisula, Entrance of the Gulf of Finlan*. Estuarine, Coastal and Shelf Science, **38**, 507-521.

Jędrasik J., 1997, *The influence of the advection on the water temperature distribution in the Gulf og Gdask; numerical study*, Oceanological Studies, No. 4, 41-64.

Killworth, P., D. Stainforth, D.J. Webbs, and S.M. Peterson, 1991, *The development of a free-surface Bryan-Cox-Semtner ocean model*, J. Phys. Oceanogr., **11**, 415-433.

Kowaleuski, M., 1997, *A three-dimensional hydrodynamic model of the Gulf of Gdask*, Oceanological Studies, **26**, No. 4, 77-98.

Krauss, W., and B. Brügge, 1991, *Wind-produced water exchange between the deep basins of the Baltic Sea,* J. Phys. Oceanogr., **21**, 373-384.

Krężel, A., 1997, *Recognition of mesoscale hydrophysical anomalies in a shallow sea using broadband satelitte teledetection methods*, Wydawnictwo Uniwersytetu Gdańskiego, Gdańsk, 173 pp. (in Polish).

Lehmann, A., 1995, *A three-dimensional baroclinic eddy-resolving model of the Baltic Sea*, Tellus, **47A**, 1013-1031.

Lehmann, A., H.H., Hinrichsen, 2000a, *On the thermohaline variability of the Baltic Sea*, Journal of Marine Systems, **25**, 333-357.

Lehmann, A., H.H., Hinrichsen, 2000b, *On the wind driven and thermohaline circulation of the Baltic Sea*, Phys. Chem. Earth (B), **25**, No. 2, 183-189.

Lenz, W., 1971, *Monatskarten der Temperatur der Ostsee, dargestellt fuer verschiedene Tiefenhorizonte*, Dt. hydrogr. Z., Erg.H.R.B., **11**, Hamburg, 148.

Meier, H.E.M, 1999, *First results of multi-year simulations using a 3D Baltic Sea model*, SMHI, Reports Oceanography, No. **27**, 48 pp.

Meier, H.E.M, R. Döscher, A.C. Coward, J. Nycander, and K. Döös, 1999 *RCO - Rossby Centre regional Ocean climate model: model description (version 1.0) and first results from the hindcast period 1992/93*, SMHI, Reports Oceanography, No. **26**, 1999, 102 pp.

Mellor, G.L., *User's guide for a three-dimensional, primitive equation, numerical ocean model*, Prog. in Atmos. and Ocean. Sci, Princeton University, 1993, 35 pp.

Mellor, G.L., and T. Yamada, 1982, *Development of a turbulent closure model for geophysical fluid problems*, Rev. Geophys., **20**, 851-875.

Mesinger, F., Arakawa, A., 1976, *Numerical models used in atmospheric models,* GARP Publications Series, No. 17, **1**, WMO-ICSU, 64.

Oey, L.Y., and P. Chen, 1992a, *A model simulation of circulation in the northeast Atlantic shelves and seas*, J. Geophys. Res., **97**, 20087-20115.

Oey, L.Y., and P. Chen, 1992b, *A nested-grid ocean model: with application to the simulation of meanders and eddies in the Norwegian coastal current*, J. Geophys. Res., **97**, 20063-20086.

Seifert, T., Kayser, B., 1995, *A high resolution spherical grid topography of the Baltic Sea*, Meereswissenschaftliche Berichte, No. **9**, Institut für Ostseeforschung, Warnemünde, 72-88.

Siegel, H., M. Gerth, R. Rudloff, and G. Tschersich, 1994, *Dynamic features in the western Baltic Sea investigated using NOAA - AVHRR Data*, Dt. hydrogr. Z., **46**, 191-209.

Smagorinsky J., 1963, *General circulatio experiments with the primitive equations. I. The basic experiment.*, Monthly Weather Reviews, 91, 99-164.

Svendsen, E., J. Berntsen, M. Skogen, B. Ådlandsvik, and E. Martinsen, 1996, *Model simulation of the Skagerrak circulation and hydrography during Skagex.* J. Mar. Systems, **8**, 219-236.

UNESCO, 1983, *Algorithms for the computation of fundamental properties of sea water*, UNESCO Tech. Pap. Mar. Sci., No. **44**.

Urbański, J., 1995, *Upwellings along the Polish coasts of the Baltic Sea*, Przegląd Geofizyczny, **XL**, 141-153 (in Polish).